universität wien

Masterarbeit / MASTER'S THESIS

Titel der Masterarbeit / Title of the Master's Thesis

Influence of mechanical stress on magnetization of iron-cobalt

verfasst von / submitted by

Emanuel Pfneisl, BSc

angestrebter akademischer Grad / in partial fulfilment of the requirements for the degree of

Master of Science (MSc)

Wien, 2019 / Vienna, 2019

Studienkennzahl lt. Studienblatt / degree programme code as it appears on the student record sheet:	UA 066 876
Studienrichtung lt. Studienblatt / degree programme as it appears on the student record sheet:	Masterstudium Physik UG2002
Betreut von / Supervisor:	Assoz. Prof. Dipl.-Ing. Dr. techn. Dieter Süss, Privatdoz.

Zusammenfassung

Magnetostriktive Eigenschaften von Materialien gewinnen in vielen Anwendungsbereichen zunehmend an Bedeutung. Vielfach aufgrund der Tatsache, dass magnetostriktive Effekte genutzt werden können um indirekt andere Größen zu messen.
Dies ist zum Beispiel bei sogenannten amorphen, magnetostriktiven Dehnungsmessstreifen der Fall: Hier werden indirekt lokale Dehnungen gemessen, indem die magnetische Antwort des Streifens gemessen wird [2]. Über die Messung der magnetischen Antwort kann bei Kenntnis der magnetostriktiven Eigenschaften des Materials auf die lokale Dehnung zurückgeschlossen werden.
Umgekehrt gibt es auch Anwendungen bei denen die Magnetostriktion einen unerwünschten Nebeneffekt darstellt, der die Messung verfälscht. Dies ist zum Beispiel bei GMR-Sensoren der Fall: Hier wird durch Magnetostriktion die Magnetisierungskurve in der weichmagnetischen Schicht (Free Layer) verändert. Die Magnetisierung des Free Layers relativ zur hartmagnetischen Schicht (Fixed Layer) ist damit beeinflusst und das Messresultat des Sensors verfälscht.
Ziel dieser Arbeit ist die Auswirkung von Magnetostriktion auf beliebige Materialien mit Hilfe der FEM-Software Magnum.fe [13] berechnen zu können.
Hierzu wird eine FEM-Formulierung zur Lösung von Elastizitätsproblemen implementiert und anschließend ein Landau-Lifschitz-Gilbert (LLG) Term für den Effekt der Magnetostriktion in kubischen Materialien hergeleitet. Als Anwendungsfall wird die spannungsabhängige Magnetisierungskurve von monokristallinem und polykristallinem Eisen-Kobalt unter dem Einfluss verschiedener Spannungszustände untersucht.
Je nach Orientierung des monokristallinem Eisen-Kobalt relativ zu der angelegten externen Spannung fällt der Effekt der Magnetostriktion unterschiedlich stark aus. Für eine externe Spannung von $0.2 \cdot \sigma_c$, angelegt auf die Probe, konnte eine Anstieg von 5% in der magnetischen Suszeptibilität festgestellt werden, wenn der Einkristall parallel zur externen Spannung ausgerichtet ist.
Die gleiche externe Spannung führt zu einem Anstieg von 64% in der magnetischen Suszeptibilität, wenn die Raumdiagonale des Einkristalls parallel zur externen Spannung ausgerichtet ist.
Für den Fall des polykristallinem Eisen-Kobalt wurde, bei der erwähnten charakteristischen Spannung, ein Anstieg von 41% in der magnetischen Suszeptibilität festgestellt.

Abstract

Magnetostrictive effects are increasingly important in a wide range of applications. There are applications were magnetostrictive effects are welcomed and actually used in order to indirectly measure other quantities. This is the case for strain gauges where amourphous magnetostrictive ribbons are used to indirectly measure a local strain by measuring the magnetic response signal which is directly related to the inner stress of the ribbon through the magneto-elastic coupling known as magnetostriction [2].
Contrarily, there are also applications were magnetostriction is an undesired side-effect. This is the case for GMR sensors where magnetostrictive effects alter the magnetization curve of the soft-magnetic layer (free layer). This results in a distorted magnetization of the free layer relative to the fixed layer and therefore measurement of the magnetic field will not be correct.
In the following work a FEM based linear elasticity solver is implemented to solve related elastic problems. Subsequently a Landau-Lifschitz-Gilbert (LLG) term for magnetostriction in cubic materials is derived and implemented. Using the micromagnetic FEM-based software magnum.fe [13] the stress-dependent magnetization curves of monocrystalline and polycrystalline iron-cobalt for different orientations of external magnetic field relative to external stress are computed. Depending on the orientation of the iron-cobalt single crystal relative to the external stresses different magnitudes of magnetostriction are observed. A specific external stress of $0.2 \cdot \sigma_c$ applied on the specimen leads to an increase in susceptibility of 5% if the single crystal is oriented parallel to the external stress. On the contrary the same external stress leads to an increase of 64% in susceptibility if the stress is aligned along the body diagonal of the single crystal. For the inhomogeneous case of randomly oriented grains an increase of 41% in susceptibility was observed.

Danksagung

An dieser Stelle möchte ich zuerst meinem Betreuer Privatdoz. Dipl.-Ing. Dr. techn. Dieter Suess für die stets hilfreiche und motivierende Betreuung meiner Masterarbeit danken.
Des weiteren gilt mein besonderer Dank meinem Ko-Betreuer Projektass. Dipl.-Ing. Dr. techn. Florian Bruckner für die vielen hilfreichen Gespräche und ausgetauschten Emails, die mich immer einen Schritt weitergebracht haben. Die Zusammenarbeit war stets konstruktiv und für mich sehr erkenntnisreich.
Einen besonders großen Dank möchte ich an meine Familie richten für die stetige Unterstützung finanzieller und emotionaler Natur. Im besonderen möchte ich mich bei meinem Bruder Sebastian Pfneisl für das akribische Korrekturlesen und das viele Feedback im Bezug auf den schriftlichen Teil der Arbeit bedanken.
Schließlich möchte ich mich noch bei Freunden und Studienkollegen für das Interesse an meiner Arbeit bedanken.

Contents

1 Introduction

Magnetostriction was first seen and studied in 1880 by J. Joule. As a simple definition magnetostriction can be seen as the deformation of a body caused by a change of magnetization. Or more abstractly and accurately expressed: magnetostriction denotes the bidirectional coupling of magnetic and elastic states. This is similar to the piezo-electric effect which is a phenomenon caused by electric-elastic coupling.
Recently magnetostrictive effects are becoming increasingly important in a wide range of applications. In some applications magnetostrictive effects are welcomed and actually used in order to indirectly measure other quantities. This for example is the case in strain gauges where amorphous magnetostrictive ribbons are used to indirectly measure a local strain by measuring the magnetic response signal which is directly related to the inner stress of the ribbon through the magneto-elastic coupling known as magnetostriction.
Contrarily, there are applications were magnetostrictive effects are an undesired by-product. This is the case for GMR sensors where magnetostrictive effects alter the magnetization curve of the soft-magnetic layer (free layer). This results in a distorted magnetization of the free layer relative to the fixed layer and therefore measurement of the magnetic field will not be correct.
This works is focused on the latter case of undesired magnetostriction in GMR sensors.
To study this effect on a microscopic level various well established techniques are used to make this complicated physical problem computationally more manageable. One of this techniques is called finite elements method (FEM) and is widely used in engineering. FEM allows to solve partial derivative equations (PDE) for complicated geometrical objects by dividing the object into smaller more manageable blocks. This process is called finite element discretization. In analogues manner the magnetization of materials can be discretized and computations can be carried out by a so-called micromagnetic approach. A macroscopic approach would equate solving the appropriate Maxwell equations.
This ideas are already implemented in the FEM-based micromagnetic python library magnum.fe [13], which is implemented on top of the FEM library FEniCS [11]. All solutions described in this work will be built as part of magnum.fe.
In order to compute the inner stress of a specimen for various boundary conditions (thermal stress, surface pressure, etc.) a rather simple solver for linear elasticity is implemented. Plastic deformatios are not considered.
In the phenomenological Landau-Lifschitz-Gilbert (LLG) micromagnetic theory magnetic effects are expressed as contributions to the total effective field. Therefore a term for the effective field of magnetostriction is derived and implemented.
Furthermore magnetization curves for various materials and boundary conditions are obtained and additionally it is studied how and where effective methods can be used to save computation time.

2 Theory

2.1 Elasticity

2.1.1 Linear Elasticity

In continuum mechanics Linear Elasticity is often used as a simplification of the more general nonlinear theory of elasticity. Using this model the following assumptions are being made [7]:

- the strains in the material are small
- stress is proportional to the strain
- material returns to it's original shape when load is removed (elastic deformation)
- stress strain relation is independent of the rate of loading or straining

In this case both stress and strain is given by a second-order tensor, σ_{ij} and ϵ_{ij}, and are related by a fourth-order tensor which is called stiffness tensor C_{ijkl} or compliance tensor S_{ijkl}:

$$\sigma_{ij} = C_{ijkl}\epsilon_{kl}$$
$$\epsilon_{ij} = S_{ijkl}\sigma_{kl}$$

This formula is often referred to as Hooke's law.
Instead of the Einstein summation convention which is used above, one could also write it in the form of a double dot product (dyadic product):

$$\sigma = C : \epsilon$$
$$\epsilon = S : \sigma$$

Tensors of stress and strain are defined as follows (see also Fig. 1):

$$\sigma = \begin{pmatrix} \sigma_{11} & \sigma_{12} & \sigma_{13} \\ \sigma_{21} & \sigma_{22} & \sigma_{23} \\ \sigma_{31} & \sigma_{32} & \sigma_{33} \end{pmatrix} = \begin{pmatrix} \sigma_{xx} & \tau_{xy} & \tau_{xz} \\ \tau_{yx} & \sigma_{yy} & \tau_{yz} \\ \tau_{zx} & \tau_{zy} & \sigma_{zz} \end{pmatrix}$$
$$\epsilon = \begin{pmatrix} \epsilon_{11} & \epsilon_{12} & \epsilon_{13} \\ \epsilon_{21} & \epsilon_{22} & \epsilon_{23} \\ \epsilon_{31} & \epsilon_{32} & \epsilon_{33} \end{pmatrix} = \begin{pmatrix} \epsilon_{xx} & \epsilon_{xy} & \epsilon_{xz} \\ \epsilon_{yx} & \epsilon_{yy} & \epsilon_{yz} \\ \epsilon_{zx} & \epsilon_{zy} & \epsilon_{zz} \end{pmatrix}$$

It can be derived from equilibrium of the forces that in linear elasticity both second-order tensors of stress and strain are inherently symmetric [14] and therefore also the fourth-order tensor connecting both has some symmetry:

$$\sigma_{ij} = \sigma_{ji} \implies C_{jikl} = C_{ijkl}$$
$$\epsilon_{ij} = \epsilon_{ji} \implies C_{ijlk} = C_{ijkl}$$

Because of this symmetries it is possible to write this important relation in the form of a simple matrix vector multiplication which is called Voigt-Notation:

$$\sigma_i = C_{ij}\epsilon_j$$

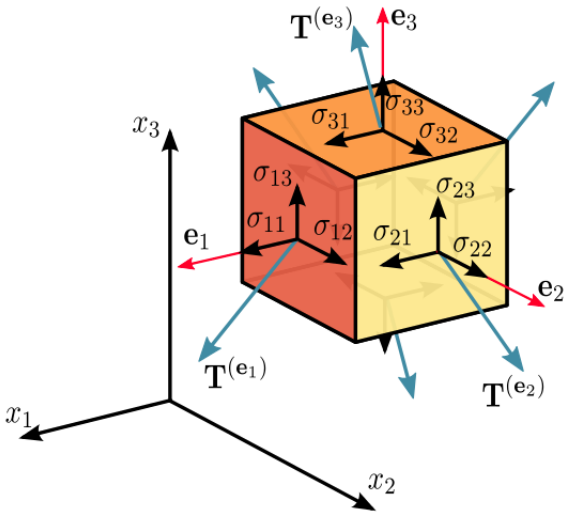

Figure 1: Geometry of stress tensor in model of linear elasticity[1]

Whereas different conventions for the definition of Voigt-Notation can be used. Commonly the following is used:

$$\sigma = \begin{pmatrix} \sigma_{11} \\ \sigma_{22} \\ \sigma_{33} \\ \sigma_{23} \\ \sigma_{13} \\ \sigma_{12} \end{pmatrix}, \epsilon = \begin{pmatrix} \epsilon_{11} \\ \epsilon_{22} \\ \epsilon_{33} \\ 2\epsilon_{23} \\ 2\epsilon_{13} \\ 2\epsilon_{12} \end{pmatrix}$$

And the fourth-order stiffness tensor is mapped upon the stiffness matrix as follows:

$$C = \begin{pmatrix} C_{1111} & C_{1122} & C_{1133} & C_{1123} & C_{1113} & C_{1112} \\ C_{2211} & C_{2222} & C_{2233} & C_{2223} & C_{2213} & C_{2212} \\ C_{3311} & C_{3322} & C_{3333} & C_{3323} & C_{3313} & C_{3312} \\ C_{2311} & C_{2322} & C_{2333} & C_{2323} & C_{2313} & C_{2312} \\ C_{1311} & C_{1322} & C_{1333} & C_{1323} & C_{1313} & C_{1312} \\ C_{1211} & C_{1222} & C_{1233} & C_{1223} & C_{1213} & C_{1212} \end{pmatrix}$$

If one further assumes a cubic material the degrees of freedom of the fourth-order tensor are reduced to three, because of symmetry reasons:

$$C = \begin{pmatrix} C_{11} & C_{12} & C_{12} & 0 & 0 & 0 \\ C_{12} & C_{11} & C_{12} & 0 & 0 & 0 \\ C_{12} & C_{12} & C_{11} & 0 & 0 & 0 \\ 0 & 0 & 0 & C_{44} & 0 & 0 \\ 0 & 0 & 0 & 0 & C_{44} & 0 \\ 0 & 0 & 0 & 0 & 0 & C_{44} \end{pmatrix}$$

And for isotropic materials only two degrees of freedom remain:

[1]Image taken from: https://de.wikipedia.org/wiki/Spannungstensor

$$C = \begin{pmatrix} C_{11} & C_{12} & C_{12} & 0 & 0 & 0 \\ C_{12} & C_{11} & C_{12} & 0 & 0 & 0 \\ C_{12} & C_{12} & C_{11} & 0 & 0 & 0 \\ 0 & 0 & 0 & (C_{11} - C_{12})/2 & 0 & 0 \\ 0 & 0 & 0 & 0 & (C_{11} - C_{12})/2 & 0 \\ 0 & 0 & 0 & 0 & 0 & (C_{11} - C_{12})/2 \end{pmatrix}$$

For this reason stiffness for isotropic materials is often given by two parameters called Lamé Constants (μ and λ):

$$C = \begin{pmatrix} \lambda + 2\mu & \lambda & \lambda & 0 & 0 & 0 \\ \lambda & \lambda + 2\mu & \lambda & 0 & 0 & 0 \\ \lambda & \lambda & \lambda + 2\mu & 0 & 0 & 0 \\ 0 & 0 & 0 & \mu & 0 & 0 \\ 0 & 0 & 0 & 0 & \mu & 0 \\ 0 & 0 & 0 & 0 & 0 & \mu \end{pmatrix}$$

Or equivalently Hooke's law for isotropic materials can be written as follows:

$$\sigma_{ij} = 2\mu\epsilon_{ij} + \lambda \mathrm{tr}(\epsilon)\delta_{ij}$$

However for anisotropy materials the stiffness matrix (or compliance matrix) is used to describe elastic properties of the material. Stiffness matrices can be found at the so-called materialsproject [6] which publishes DFT (Density Functional Theory) derived stiffness matrices which can be used freely.
According to the materialsproject derived stiffness matrices are within 15% of experimental values [4].
For iron-cobalt (FeCo) the following stiffness matrix is used:

$$C = \begin{pmatrix} 259 & 154 & 154 & 0 & 0 & 0 \\ 154 & 254 & 154 & 0 & 0 & 0 \\ 154 & 154 & 254 & 0 & 0 & 0 \\ 0 & 0 & 0 & 131 & 0 & 0 \\ 0 & 0 & 0 & 0 & 131 & 0 \\ 0 & 0 & 0 & 0 & 0 & 131 \end{pmatrix} GPa$$

And a compliance matrix of:

$$S = \begin{pmatrix} 6.9 & -2.6 & -2.6 & 0 & 0 & 0 \\ -2.6 & 6.9 & -2.6 & 0 & 0 & 0 \\ -2.6 & -2.6 & 6.9 & 0 & 0 & 0 \\ 0 & 0 & 0 & 7.6 & 0 & 0 \\ 0 & 0 & 0 & 0 & 7.6 & 0 \\ 0 & 0 & 0 & 0 & 0 & 7.6 \end{pmatrix} 10^{-12} Pa^{-1}$$

2.1.2 Elastic moduli

Instead of the generalized stiffness matrix commonly several specific ratios of stress and strain are used to characterize materials (see also Fig. 2). The three most important elastic moduli are:

- Young's modulus (also called E-modulus)
- Shear modulus
- Bulk modulus
- Poisson ratio

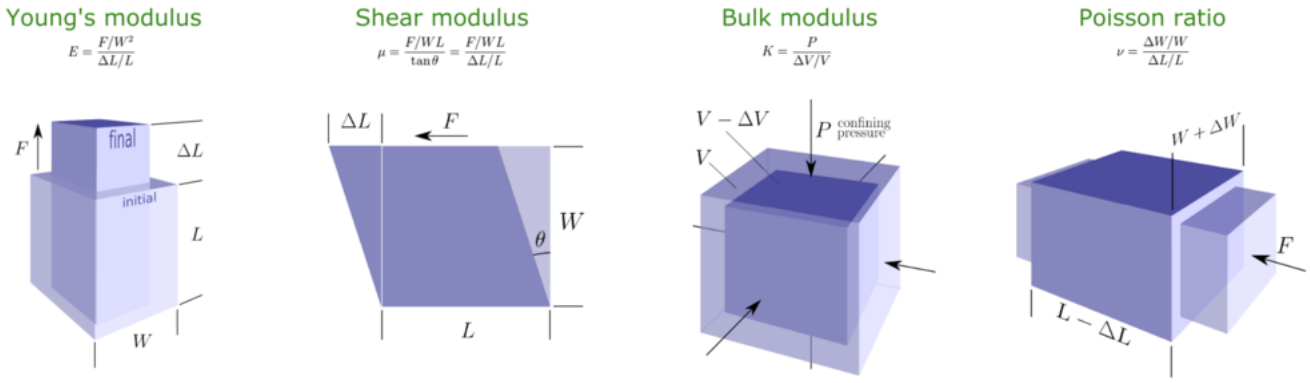

Figure 2: Elastic moduli in linear elasticity[2]

For this reason an isotropic stiffness can be written in terms of the elastic moduli:

$$C = \frac{E}{(1+\nu)(1-2\nu)} \begin{pmatrix} 1-\nu & \nu & \nu & 0 & 0 & 0 \\ \nu & 1-\nu & \nu & 0 & 0 & 0 \\ \nu & \nu & 1-\nu & 0 & 0 & 0 \\ 0 & 0 & 0 & \frac{1-2\nu}{2} & 0 & 0 \\ 0 & 0 & 0 & 0 & \frac{1-2\nu}{2} & 0 \\ 0 & 0 & 0 & 0 & 0 & \frac{1-2\nu}{2} \end{pmatrix}$$

For anisotropic materials these moduli are obviously directional dependent and can be visualized in a three-dimensional plot as seen in Fig. 3. For an isotropic material this visualisation would simply be a sphere.

[2]Image taken from: https://agilescientific.com/blog/2016/4/28/all-the-elastic-moduli
[3]Image taken from open source tool ELATE: http://progs.coudert.name/elate/mp?query=mp-2090

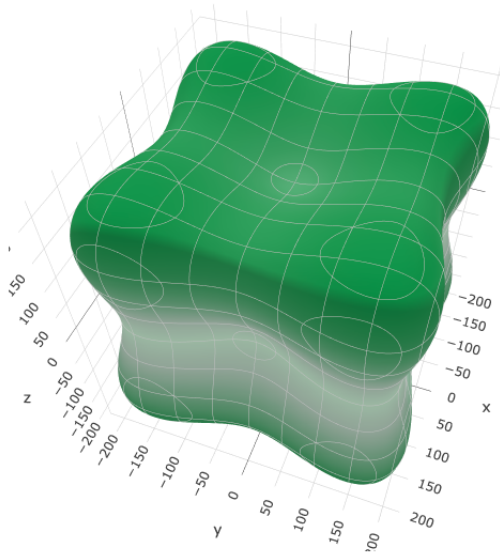

Figure 3: Spatial dependence of Young's modulus for FeCo visualized in 3D plot using open source software ELATE[3]

2.1.3 PDE Problem and variational formulation

In linear elasticity deformations of a body Ω are given by the following partial differential equation:

$$-\nabla \cdot \sigma = f_{vol} \text{ in } \Omega$$

Whereas f_{vol} is the body force per volume unit.

According to Hooke's law the stress tensor can be expressed in terms of stiffness and strain tensor:

$$\sigma_{ij} = C_{ijkl}\epsilon_{kl}$$

And further the strain tensor is given by the displacement vector field u:

$$\epsilon = \frac{1}{2}(\nabla u + (\nabla u)^T)$$

Combined this results in (written as dyadic product):

$$-\frac{1}{2}\nabla \cdot \left[C : (\nabla u + (\nabla u)^T\right] = f_{vol}$$

A variational formulation is obtained by forming the inner product of this equation and a vectorial test function v:

$$-\int_\Omega (\nabla \cdot \sigma) \cdot v \, dx = \int_\Omega f_{vol} \cdot v \, dx$$

Since there are second-order derivatives on the left-hand-side integration by parts is used:

$$-\int_\Omega (\nabla \cdot \sigma) \cdot v \, dx = \int_\Omega \sigma : \nabla v \, dx - \int_{\partial\Omega} (\sigma \cdot n) \cdot v \, ds$$

Here n is the outward normal on the boundary. Therefore $\sigma \cdot n$ is a stress vector at the boundary. Usually this is given as a boundary condition $T = \sigma \cdot n$ on a specific part of the boundary $\partial\Omega_T$

(the remaining part is given by dirichlet condition). It follows:

$$\int_\Omega \sigma : \nabla v \, dx = \int_\Omega f_{vol} \cdot v \, dx + \int_{\partial\Omega_T} T \cdot v \, ds$$

Summarized the variational formulation is given as:

$$a(u, v) = L(v) \quad \forall v \in \hat{V} \tag{1}$$

Whereas:

$$a(u, v) = \int_\Omega \sigma(u) : \nabla v \, dx, \tag{2}$$

$$\sigma(u) = \frac{1}{2}\big(\nabla u + (\nabla u)^T\big) : C \tag{3}$$

$$L(v) = \int_\Omega f_{vol} \cdot v \, dx + \int_{\partial\Omega_T} T \cdot v \, ds \tag{4}$$

2.1.4 Effective elastic moduli

In practice mostly polycrystalline materials are used because they are more simple to produce. Polycrystalline materials are composed of a large number of grains. A grain is a volume element having the same orientation. The sum and distribution of those grains is called the texture of the material.
In order to calculate the effective elastic moduli analytically one first of all has to be able to rotate the fourth-order tensor according to the respective grain. This can be achieved by applying a conventional rotation matrix for each order successively:

$$C'_{ijkl} = C_{mnop} R_{lp} R_{ko} R_{jn} R_{im}$$

If one considers an anisotropic material with uniform randomly oriented grains the effective stiffness can be analytically solved by taking the average of stiffness or compliance tensor.
This is only valid if one assumes no interaction of grains at all. Further there are two possible ways to take the average. Either the average of stiffness is taken - this is called Voigt Method. Here implicitly a constant strain is assumed. Or alternatively the average of compliance is taken - this is called Reuss Method. Here implicitly a constant stress is assumed [10].

Voigt Method

$$\bar{C}_{ijkl} = \int_{all\ possible\ R} C_{mnop} R_{lp} R_{ko} R_{jn} R_{im}$$

For cubic materials this results in the following so-called Voigt effective elastic constants:

$$E_V = \frac{(C_{11} - C_{12} + 3C_{44})(C_{11} + 2C_{12})}{2C_{11} + 3C_{12} + C_{44}}, G_V = \frac{C_{11} - C_{12} + 3C_{44}}{5}, \nu_V = \frac{C_{11} + 4C_{12} - 2C_{44}}{4C_{11} + 6C_{12} + 2C_{44}}$$

Corresponding Lamé constants are given by:

$$\begin{aligned} \mu &= \frac{1}{5}(C_{11} - C_{12} + 3C_{44}) \\ \lambda &= \frac{(C_{11} + 4C_{12} - 2C_{44})(C_{11} - C_{12} + 3C_{44})}{5(3C_{11} + 7C_{12} - C_{44})} \end{aligned} \tag{5}$$

Reuss Method

$$\bar{S}_{ijkl} = \int_{all\ possible\ R} S_{mnop} R_{lp} R_{ko} R_{jn} R_{im}$$

For cubic materials this results in the following so-called Reuss effective elastic constants:

$$E_R = \frac{5}{3S_{11} + 2S_{12} + S_{44}}, G_R = \frac{5}{4S_{11} - 4S_{12} + 3S_{44}}, \nu_R = -\frac{2S_{11} + 8S_{12} + S_{44}}{6S_{11} + 4S_{12} + 2S_{44}}$$

Corresponding Lamé constants are given by:

$$\begin{aligned} \mu &= \frac{5}{8S_{11} + 12S_{12} + S_{44}} \\ \lambda &= \frac{2S_{11} + 8S_{12} - S_{44}}{(S_{11} + 2S_{12})(8S_{11} + 12S_{12} + S_{44})} \end{aligned} \tag{6}$$

Empirically it has been shown that these methods yield upper and lower bounds of the actual effective elasticity. Therefore taking the mean of both yields good results. This method is called Hill Method:

$$E_H = \frac{E_R + E_V}{2}, G_H = \frac{G_R + G_V}{2}, \nu_H = \frac{E_H}{2G_H} - 1 \tag{7}$$

2.2 Magnetostriction

2.2.1 Magnetoelasticity

It is well-known that ferromagnetic materials experience a change in shape when an external magnetic field is applied. Or more formally speaking, magnetostriction describes the fact that magnetic field and elastic strain are coupled. For this reason the term magnetoelasticity is often used.
This effect is responsible for the low-pitched humming sound which transformators emit when connecting to an oscillating AC source. In this case oscillating currents produce an oscillating magnetic flux which results in oscillating elastic strain and therefore propagation of sound waves. The inverse effect, in which elastic strain (or elastic stress) results in a change of magnetization is called Villari Effect.

2.2.2 Isotropic magnetostriction

As soon as an isotropic material is considered magnetic it already suffers from a change in volume because of an effect called volume magnetostriction which is quantified by the volume magnetostriction coefficient $\lambda^{\alpha,0}$ [5].
If a magnetic field H is applied upon this magnetic isotropic material, a strain in the direction of the field, given by $\lambda_{\parallel}$, and perpendicular to the field, given by $\lambda_{\perp}$, is measured.
Since this change of length is volume conserving it follows for technical saturation:

$$\lambda_{\parallel} = -2\lambda_{\perp} = \lambda_s$$

This defines saturation magnetostriction for isotropic materials. Given that λ_s can be both positive and negative, there are already two modes for magnetostriction in isotropic materials (see Fig. 4).

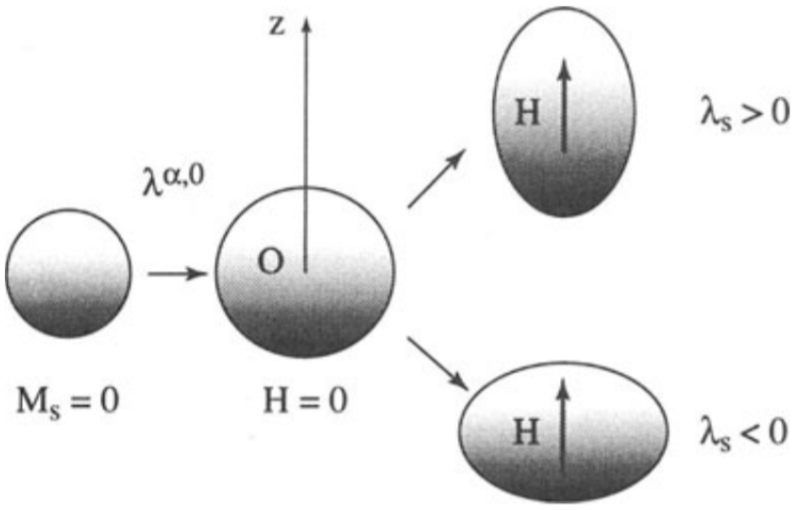

Figure 4: Volume magnetostriction and two modes of magnetostriction in isotropic materials when magnetic field is applied[4].

[4]Image taken from [5]

2.2.3 Magnetostriction for cubic symmetry

In order to find an expression for magnetostriction of cubic materials one has to firstly express elastic energy and magnetoelastic energy and then minimize the sum of those energies.
In a formalism introduced by Callen[5] the energies are approximated by the following second-order expressions:
Magnetoelastic energy:

$$E_{mel} = \frac{B^{\alpha}}{3}(\epsilon_{xx}+\epsilon_{yy}+\epsilon_{zz}) + B^{\gamma,2}\left[\frac{2}{3}\Big(\epsilon_{zz}-\frac{\epsilon_{xx}+\epsilon_{yy}}{2}\Big)\Big(m_z^2-\frac{m_x^2+m_y^2}{2}\Big)+\frac{1}{2}(\epsilon_{xx}-\epsilon_{yy})(m_x^2-m_y^2)\right]$$
$$+2B^{\epsilon,2}(\epsilon_{yz}m_y m_z+\epsilon_{zx}m_z m_x+\epsilon_{xy}m_x m_y)$$

Here m_x, m_y, m_z refers to the reduced magnetization, B^{α}, $B^{\gamma,2}$, $B^{\epsilon,2}$ are the magnetoelastic coupling constants, whereas the notation is based on symmetry group considerations [5] and ϵ refers to the strain tensor.

Elastic energy:

$$E_{el} = \frac{1}{2}c^{\alpha}\frac{1}{3}\big(\epsilon_{xx}+\epsilon_{yy}+\epsilon_{zz}\big)^2+\frac{1}{2}c^{\gamma}\left[\frac{2}{3}\Big(\epsilon_{zz}+\frac{\epsilon_{xx}+\epsilon_{yy}}{2}\Big)^2+\frac{1}{2}\big(\epsilon_{xx}-\epsilon_{yy}\big)^2\right]+c^{\epsilon}\Big(\epsilon_{yz}^2+\epsilon_{zx}^2+\epsilon_{xy}^2\Big)$$

Here c^{α}, c^{γ} and c^{ϵ} refers to the stiffness tensor components. Whereas the notation is again based on symmetry group considerations [5]. Minimizing the sum of those energies shows that magnetostriction is given by the six components of strain:

$$\begin{aligned}
\epsilon_{xx}+\epsilon_{yy}+\epsilon_{zz} &= -\frac{B^{\alpha}}{c^{\alpha}}\\
\epsilon_{zz}-\frac{\epsilon_{xx}+\epsilon_{yy}}{2} &= -\frac{B^{\gamma,2}}{c^{\gamma}}\Big(m_z^2-\frac{m_x^2+m_y^2}{2}\Big)\\
\epsilon_{xx}-\epsilon_{yy} &= -\frac{B^{\gamma,2}}{c^{\gamma}}\big(m_x^2-m_y^2\big)\\
\epsilon_{yz} &= -\frac{B^{\epsilon,2}}{c^{\epsilon}}m_y m_z\\
\epsilon_{zx} &= -\frac{B^{\epsilon,2}}{c^{\epsilon}}m_z m_x\\
\epsilon_{xy} &= -\frac{B^{\epsilon,2}}{c^{\epsilon}}m_x m_y
\end{aligned}$$

Magnetostriction coefficients are then defined by:

$$\lambda^{\alpha,0} = -\frac{B^{\alpha}}{c^{\alpha}},\ \lambda^{\gamma,2} = -\frac{B^{\gamma,2}}{c^{\gamma}},\ \lambda^{\epsilon,2} = -\frac{B^{\epsilon,2}}{c^{\epsilon}}$$

There are certainly higher-orders terms of magnetostriction but these can be neglected because they are reasonable small especially at room temperature.
Therefore magnetostriction can be described by a fourth-order tensor which is defined by two coefficients:

$$\epsilon = \lambda : (mm^T)$$

or

$$\epsilon_{ij}^{m} = \begin{cases} \frac{3}{2}\lambda_{100} m_i m_j, & i = j \\ \frac{3}{2}\lambda_{111} m_i m_j, & i \neq j \end{cases}$$

Volume magnetostriction is neglected here because we are only interested in relative anisotropic expansion.
Now strain can be expressed in terms of elastic and magnetic contributions:

$$\epsilon = \epsilon^{el} + \epsilon^{m}$$

And elastic energy therefore written as [9]:

$$E_{el} = \frac{1}{2}\big(\epsilon - \epsilon^{m}(\vec{m})\big) : C : \big(\epsilon - \epsilon^{m}(\vec{m})\big)$$

In order to obtain the effective magnetic field $\vec{H}_{eff}$ the functional derivation with respect to the reduced magnetization has to be taken. This results in:

$$\vec{H}_{eff} = -\frac{1}{\mu_0 M_s}\frac{\partial E}{\partial \vec{m}} = \frac{1}{\mu_0 M_s} C \left(\epsilon - \epsilon^{m}(\vec{m})\right) \cdot \frac{\partial \epsilon^{m}(\vec{m})}{\partial \vec{m}}$$

Please note that the prefactor $\frac{1}{2}$ of elastic energy and the minus sign in the definition of effective field vanishes because of taking the derivative.
In the next step another approximation is done and the absolute strain $\epsilon^{m}(\vec{m})$ is neglected but partial derivative of $\epsilon^{m}(\vec{m})$ is still considered:

$$\vec{H}_{eff} = \frac{1}{\mu_0 M_s} C \left(\epsilon - \cancel{\epsilon^{m}(\vec{m})}\right) \cdot \frac{\partial \epsilon^{m}(\vec{m})}{\partial \vec{m}}$$

Therefore using Hook's law the effective field can be expressed in terms of stress σ:

$$\vec{H}_{eff} = \frac{1}{\mu_0 M_s} \sigma : \frac{\partial \epsilon^{m}(\vec{m})}{\partial \vec{m}}$$

In order to take the functional derivative of $\epsilon^{m}(\vec{m})$ in respect to $\vec{m}$ analytically the symmetry of magnetostriction tensor is used as shown by A. Visintin [15]:

$$\lambda_{ijpg} = \lambda_{ijqp}$$

Therefore, the endresult for the effective magnetic field as it will be used in the phenomenological Landau-Lifschitz-Gilbert (LLG) micromagnetic theory is simply:

$$H_{eff,k} = \frac{2}{\mu_0 M_s} \sigma_{ij} \lambda_{ijkq} m_q \tag{8}$$

Please note the prefactor 2 which is a consequence of using the symmetry of magnetostriction tensor as shown by A. Visintin [15].
Overall for imagination purposes there is a very elegant way of expressing the energy contribution from magnetostriction [8]:

$$E_{el} = -\frac{3}{2}\lambda_{100}\sum_{i=1}^{3}\sigma_{ii}M_i^2 - \frac{3}{2}\lambda_{111}\sum_{i\neq j}^{3}\sigma_{ij}M_i M_j$$

It is important to note that this formula implicitly assumes a single crystal oriented parallel to

coordinate system.
Also it is apparent that the second term vanishes, if there are no shear stresses.

For thin FeCo films, as there are used in GMR sensors, the following magnetostriction constants are used [3]:

$$\lambda_{100} = 18 \cdot 10^{-6}$$
$$\lambda_{111} = 101 \cdot 10^{-6}$$

2.2.4 Effective magnetostriction

Similar to elasticity also magnetostriction is coupled to the crystal structure. Therefore polycrystalline materials can be described by effective constants according to the texture of the material. Since magnetostriction - as derived in the previous sections - is sufficiently described by two magnetostriction coefficients this problem is much simpler:
Usually in the case of uniform randomly oriented grains saturation magnetostriction is used.
Instead of a material consisting of uniform randomly oriented grains one can aquivalently consider one single grain and sum over all possible direction.
This approximation is only valid when [5]:

- Magnetostriction constants λ_{100} and λ_{111} have the same sign and similar order of magnitude
- Elastic constants are fairly isotropic
- Polycrystalline material has no texture (grains are uniform randomly oriented)

This results in the following expression for saturation magnetization:

$$\lambda_s = \frac{4}{15}\lambda_{111} + \frac{2}{5}\lambda_{100}$$

Alternatively one can calculate an effective magnetostriction by summing over all possible direction and effectively building the average of the fourth-order magnetostriction tensor λ. This can be done similar to effective stiffness by using Voigt, Reuss or Hill-Method.

2.2.5 Uniaxial anisotropy

Many magnetic effects in cubic materials can be expressed in the form of a cubic anisotropy.
However if one assumes uniaxial stress it is possible to express magnetostriction in the form of an uniaxial anisotropy.
A second-order uniaxial anisotropy can be written as:

$$\vec{H} = \frac{2\,K_{uni}}{\mu_0\,M_s}\vec{K}_{axis}(\vec{K}_{axis} \cdot\ \vec{m})$$

Here $\vec{K}_{axis}$ denotes the anisotropy axis (direction of least energy) and K_{uni} the anisotropy constant.
In case of a single cubic crystal and an applied stress along the crystal axis x, $\vec{K}_{axis}$ simply points in the direction of x and the K_{uni} is given by:

$$K_{uni} = \frac{3}{2}\lambda_{100}\sigma_{xx}$$

Whereas σ_{xx} equals the applied stress in the direction of x.

In case of a polycrystalline material an effective magnetostriction has to be used. Commonly the saturation magnetostriction is used but also other approximations of effective magnetostriction can be used as seen in section 2.2.4. In that case the following expression for K_{uni} is used:

$$K_{uni} = \frac{3}{2}\lambda_s \sigma$$

Whereas σ refers to the applied stress and $\vec{K}_{axis}$ point in the direction of this stress. This relation is also used in the analytical model derived by B. Bergmair [2].

3 Results

Most of the following sections are also implemented as unit tests in magnum.fe.

3.1 Simple deformations (Elastic moduli)

In a first step the deformation of a simple cubic body is solved.
For this a fixed stiffness matrix of iron-cobalt (FeCo) is used and boundary conditions are applied: the lower face is fixed by dirichlet conditions and on the upper face a compressive stress is applied. Resulting deformations for different pressures are shown in Fig. 5. As a simple check the change of expansion in direction of applied stress and in perpendicular direction is measured and from this elastic moduli are calculated (denoted by Young's modulus $E_{measured}$ and Poisson's ratio $\nu_{measured}$).
Elastic moduli have to conform with values directly calculated out of stiffness tensor of the specific material (E_{calc} and ν_{calc}).
Results for different stresses and average relative expansion parallel and perpendicular to the applied stress are as follows:

Compressive stress	$E_{measured}$	$\nu_{measured}$	$\epsilon_{\parallel}$	$\epsilon_{\perp}$
10 GPa	156.14 GPa	2.994	-0.6%	0.2%
20 GPa	156.14 GPa	2.994	-1.3%	0.4%
30 GPa	156.14 GPa	2.994	-1.9%	0.6%
40 GPa	156.14 GPa	2.994	-2.6%	0.9%

Stiffness and compliance matrix of FeCo in Voigt notation is given by:

$$C = 10^9 Pa \cdot \begin{pmatrix} 259 & 154 & 154 & 0 & 0 & 0 \\ 154 & 259 & 154 & 0 & 0 & 0 \\ 154 & 154 & 259 & 0 & 0 & 0 \\ 0 & 0 & 0 & 131 & 0 & 0 \\ 0 & 0 & 0 & 0 & 131 & 0 \\ 0 & 0 & 0 & 0 & 0 & 131 \end{pmatrix}$$

$$S = 10^{-12} Pa^{-1} \cdot \begin{pmatrix} 6.9 & -2.6 & -2.6 & 0 & 0 & 0 \\ -2.6 & 6.9 & -2.6 & 0 & 0 & 0 \\ -2.6 & -2.6 & 6.9 & 0 & 0 & 0 \\ 0 & 0 & 0 & 7.6 & 0 & 0 \\ 0 & 0 & 0 & 0 & 7.6 & 0 \\ 0 & 0 & 0 & 0 & 0 & 7.6 \end{pmatrix}$$

Considering Hooke's law it is very simple to calculate Young's modulus and Poisson's ratio analytically for this specific case. Here the stress tensor σ consists only of one entry σ_{22} which is the applied stress. Therefore:

$$E_{calc} = \frac{1}{s_{22}} = 144.93 GPa$$
$$\nu_{calc} = -\frac{s_{22}}{s_{12}} = 2.65$$

The comparison of those values with simulated values shows 8% deviation in terms of Young's Moduli and 13% in terms of poisson's ratio.

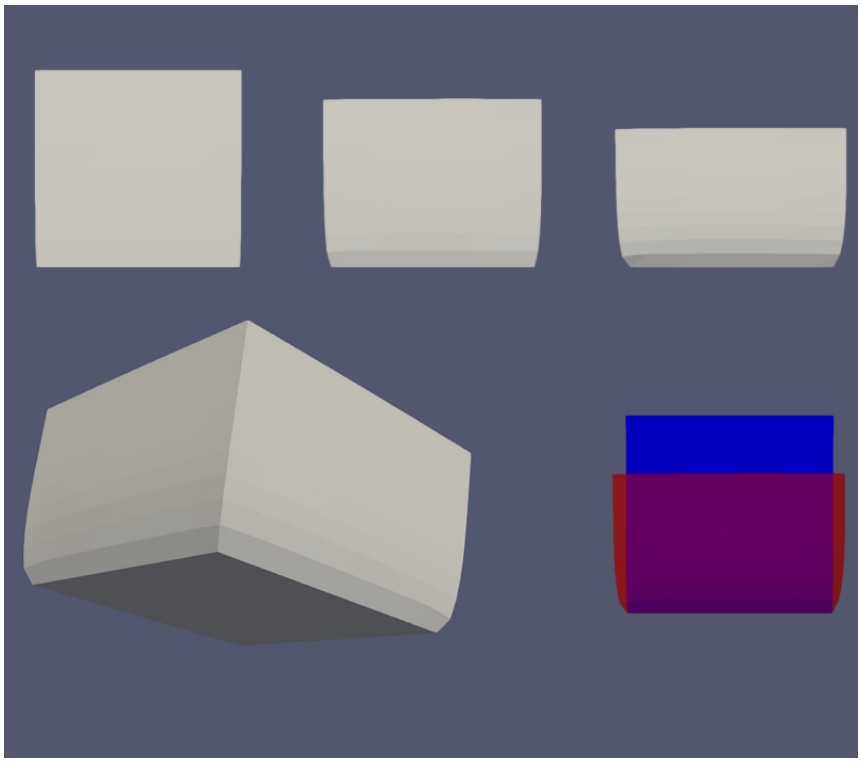

Figure 5: Deformations for 10GPa, 50GPa and 100GPa as produced by the elasticity solver (Eq. 1-4). Poisson's ratio can be seen on bottom-right (blue=10Gpa, red=100GPa).

3.2 Inner stress formation

When a stress is applied on one face and the opposite face is fixed an inhomogeneous inner stress is established as seen in Fig. 6.
On the other hand if a force is applied on both faces in a compressive manner a homogeneous inner stress is established as seen in Fig. 7.
The latter case resembles the deformation which is caused in the case of thermal expansion for example.
If this is the case a constant stress can be assigned throughout the whole mesh and no boundary conditions or linear elasticity solver has to be used.

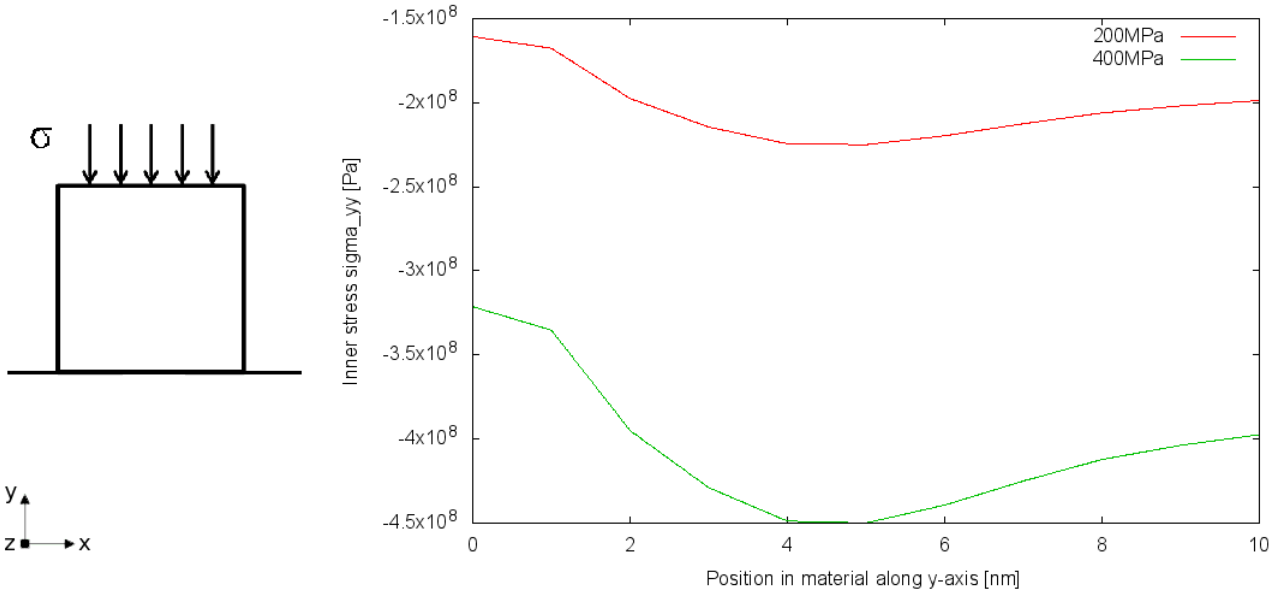

Figure 6: Inner stress of two separate cubes. Bottom (y=0) is fixed with Dirichlet boundary conditions on the top a force of 200MPa and 400MPa respectively is applied (Eq. 1-4 for linear elasticity are solved)

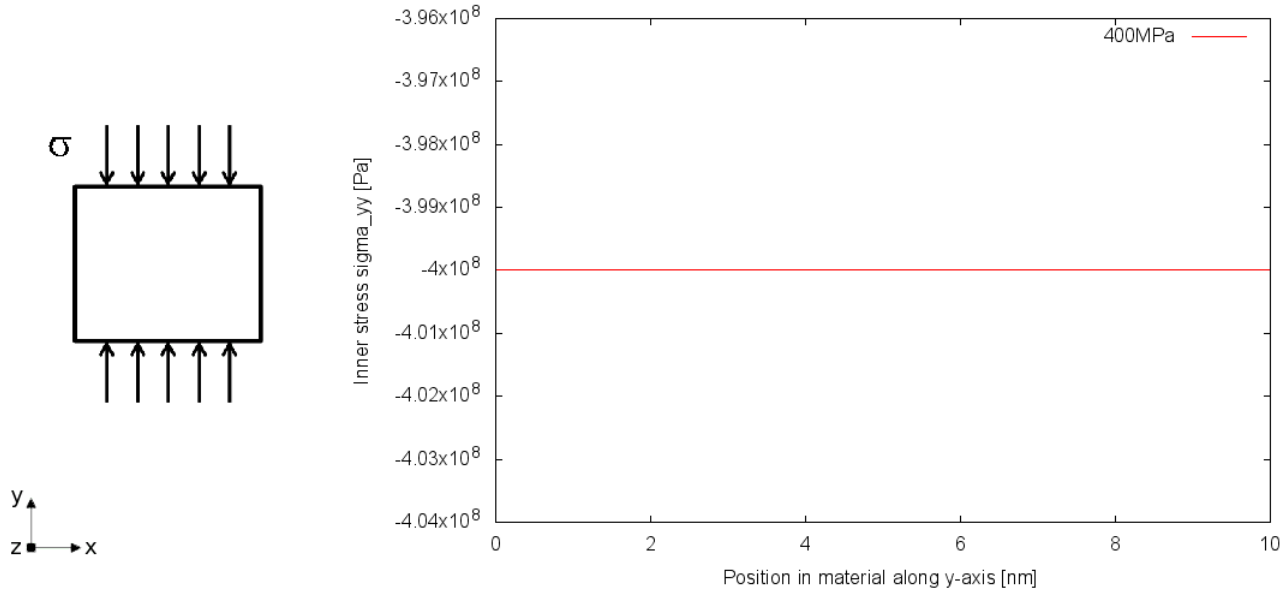

Figure 7: Inner stress of a cube. On both sides a force of 400MPa is applied in a compressive manner. A constant stress is established.

3.3 Influence of geometry: long rod

As seen in Fig. 6 inner stress in a cube varies significantly throughout the cube and this gets worse if bigger forces are applied as seen for 400MPa which is the yield strength (end of elastic region) of FeCo.
In order to see if this gets worse for different geometries the same elastic problem is solved for a long rod (see Fig. 8).

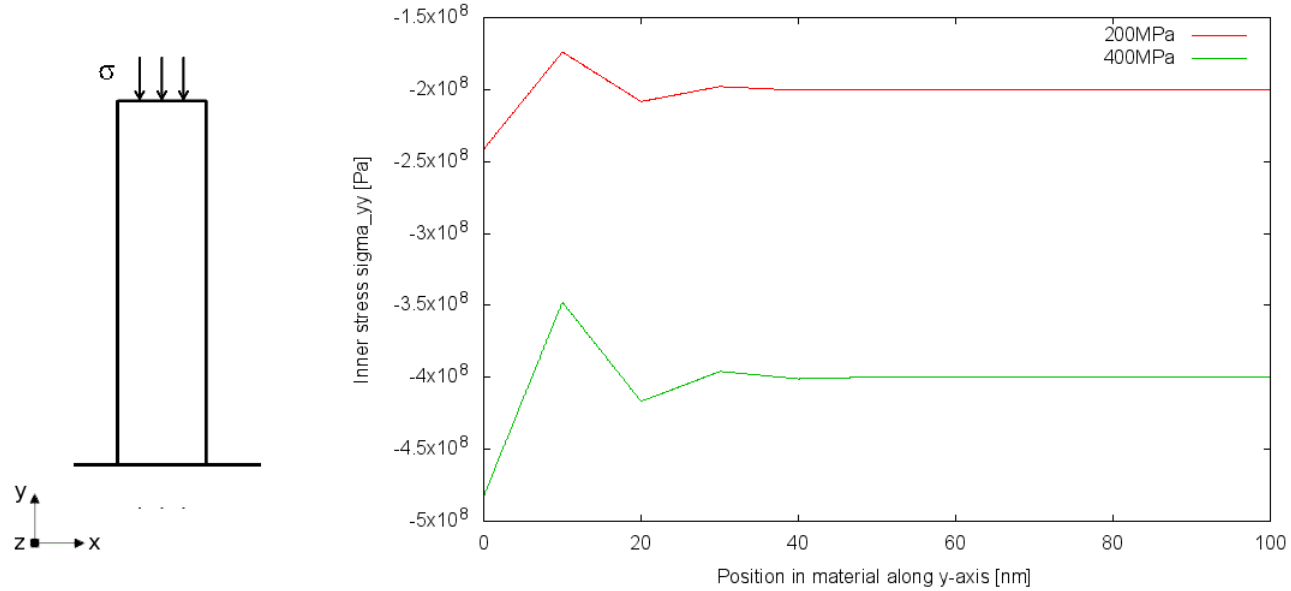

Figure 8: Inner stress of a long rod. Bottom (y=0) is fixed, on the top a force of 200MPa and 400MPa respectively is applied (Eq. 1-4 for linear elasticity are solved).

Similar to the compressed cube, a compressed long rod with the same force applied on both sides

again shows a constant inner stress as seen in Fig. 9.

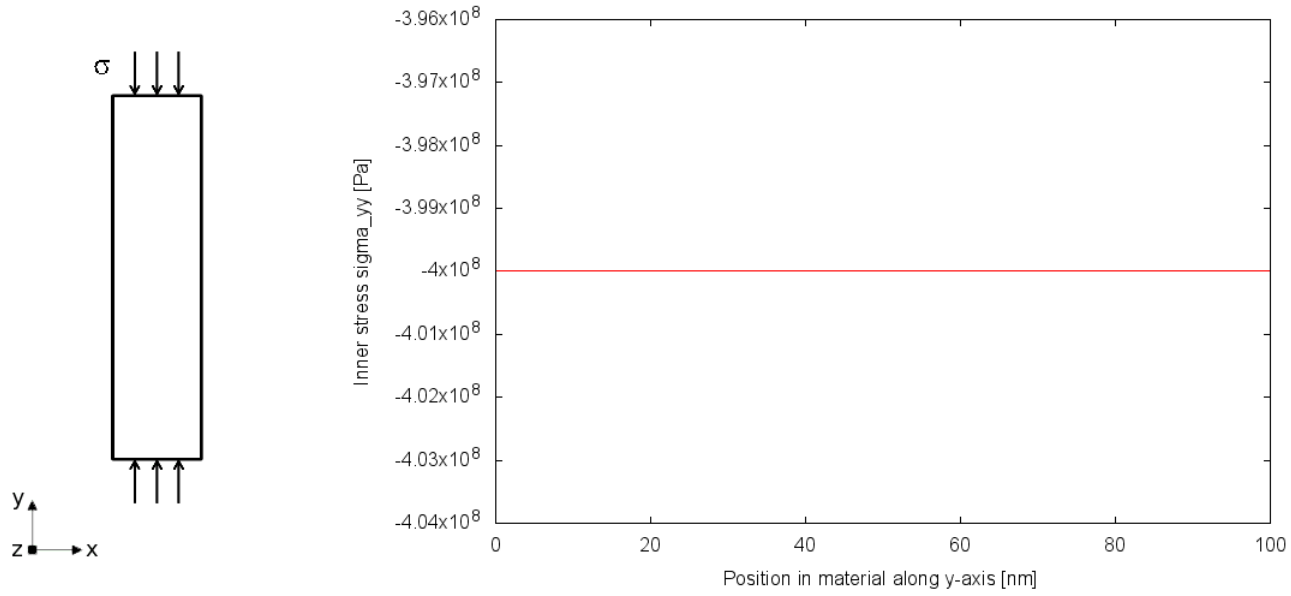

Figure 9: Inner stress of a long rod. On both sides a force of 400MPa is applied in a compressive manner. A constant stress is established (Eq. 1-4 for linear elasticity are solved).

3.4 Effective elastic moduli (Reuss, Voigt, Hill)

As discussed in section 2.1.4 commonly polycrystalline materials are used in practice. Therefore a mesh with randomly oriented grains has to be build [1] and a respectively rotated stiffness tensor has to be assigned to each grain. Then the elastic problem can be solved as usual.
A typical grain structure is shown in Fig. 10. Rotations of stiffness tensors are done according to the following random angles:

$$\begin{aligned} \theta &= 2\pi \cdot \xi' \\ \phi &= arccos(1 - 2 \cdot \xi'') \\ \alpha &= 2\pi \cdot \xi''' \end{aligned} \tag{9}$$

Here ξ', ξ'' and ξ''' are random numbers between 0 and 1.
The angles θ and ϕ define the normalized random rotation axis by the following vector:

$$\vec{r} = \begin{pmatrix} \sin\phi\cos\theta \\ \sin\phi\sin\theta \\ \cos\phi \end{pmatrix}$$

Together with the random angle α a rotation matrix is built using the exponential definition of rotation matrices:

$$R = \exp(\mathbb{1} \cdot \alpha\vec{r})$$

Subsequently the rotation matrix is applied upon the respective stiffness tensor of each grain:

$$C'_{ijkl} = C_{mnop}R_{lp}R_{ko}R_{jn}R_{im}$$

Figure 10: Example for a grain structure used in simulations. Different colors represent different domains.

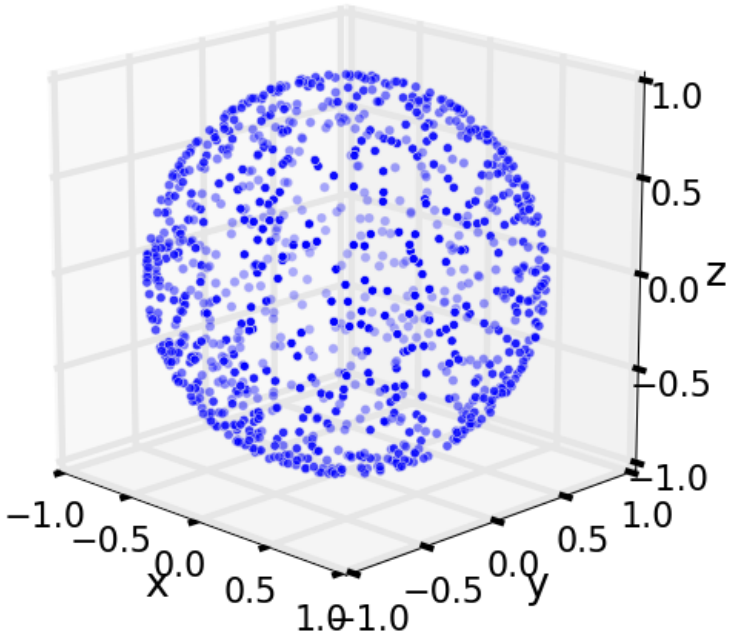

Figure 11: Blue points shows angular distribution of grain orientation as generated by Eq. 9. Cleary a uniform distribution is established [5].

This results in uniform distributed orientations on a sphere surface.

In order to compare the elastic moduli of a polycrystalline material with the various analytical solutions mentioned in Section 2.1.4, a simple elastic problem (with grain structure) is formulated and Young's modulus is measured.
Materials with various degrees of anisotropy are used to get an overview about the accuracy of analytical solutions.
The analytical solution according to Reuss seems to best fit the solution of the implemented solver across all tested materials. Therefore, for simple problems a homogeneous mesh (without domains) with an effective stiffness tensor can be used which is much more efficient.
Results are shown in Fig. 12.

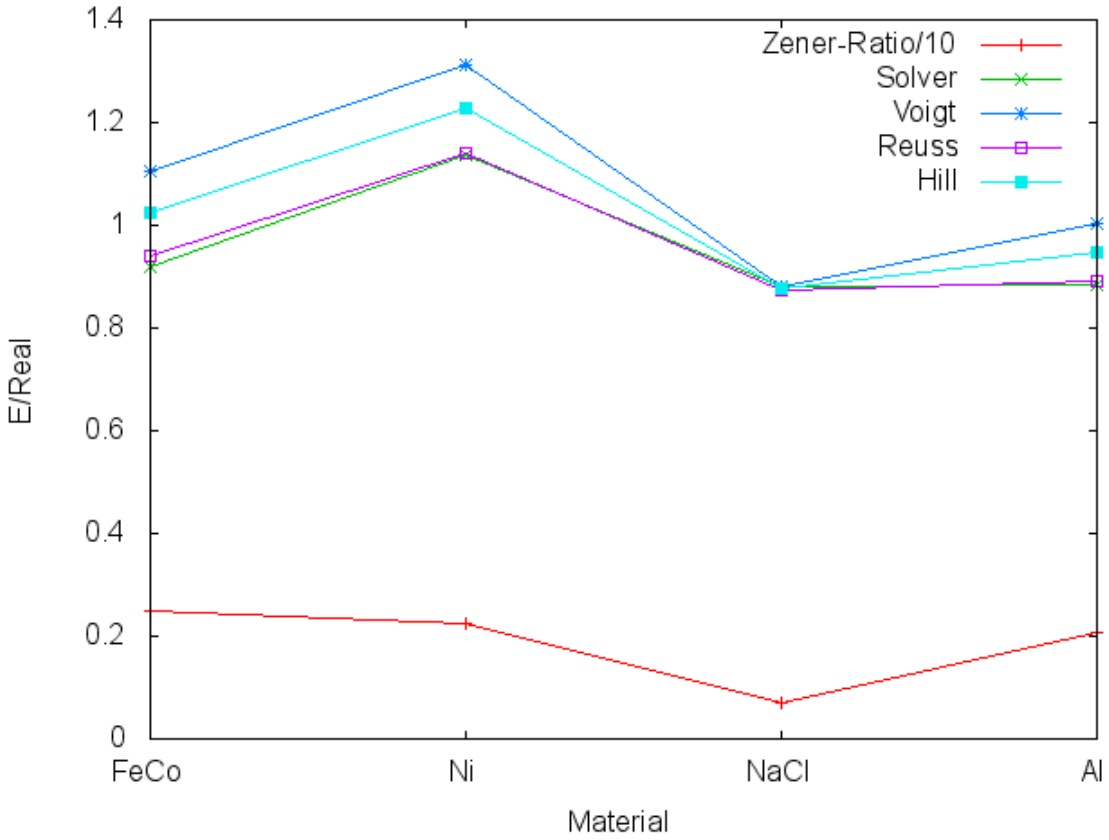

Figure 12: Young's moduli are divided by literature values to better visualize results for different materials. Zener-Ratio is included as a measure of anisotropy for the respective material. "Solver" corresponds to solving Eq. 1-4 for individually randomly oriented grains. For "Voigt", "Reuss" and "Hill" a homogen mesh with effective stiffness constants is used. See Eq. 5, 6 and 7.

3.5 Inner stress formation for grain structure

As shown in the previous section it is possible to use an effective stiffness tensor to approximate the behaviour of a polycrystalline material. But magnetostriction might be sensible to fluctuations of stress inside the structure. For this reason similar to Section 3.2 some simple elastic problems are solved and inner stress is obtained.
Firstly a stress is applied on one side of a mesh on the other side is fixed through dirichlet boundary conditions.
In contrast to section 3.2 a grain structure with randomly oriented grains is used. Results are similar (see Fig. 13) to the case of using a homogeneous mesh but with additional strong fluctuations because of the randomly oriented grains.
Secondly a stress is applied on both sides in a compressive manner similar results are obtained (see Fig. 14).
Therefore, in case of grain structure the elasticity solver has to be used in every case since no constant stress is established and fluctuations are too strong to be neglected.
This fluctuations are visible in the displacement field as shown in Fig. 15 and also in the stress tensor field (see Fig. 16). .

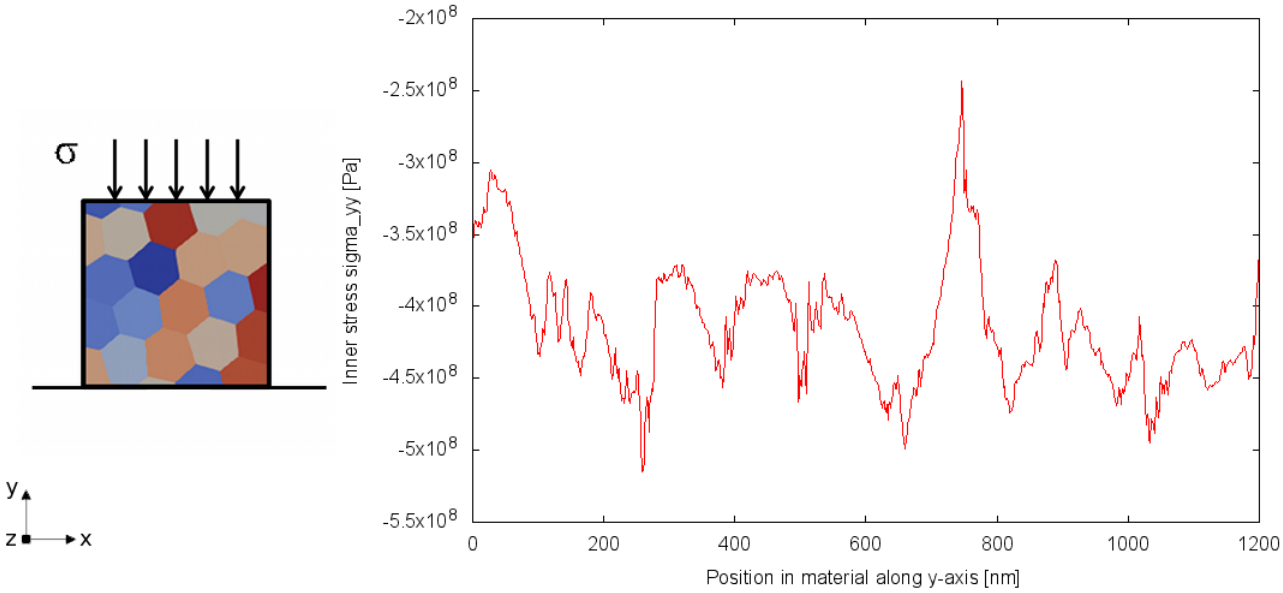

Figure 13: Inner stress of a grain structure with randomly oriented grains. Here the left side is fixed, on the right side a force of 400MPa is applied. Eq. 1-4 for linear elasticity are solved.

[5]Image taken from: http://corysimon.github.io/articles/uniformdistn-on-sphere/

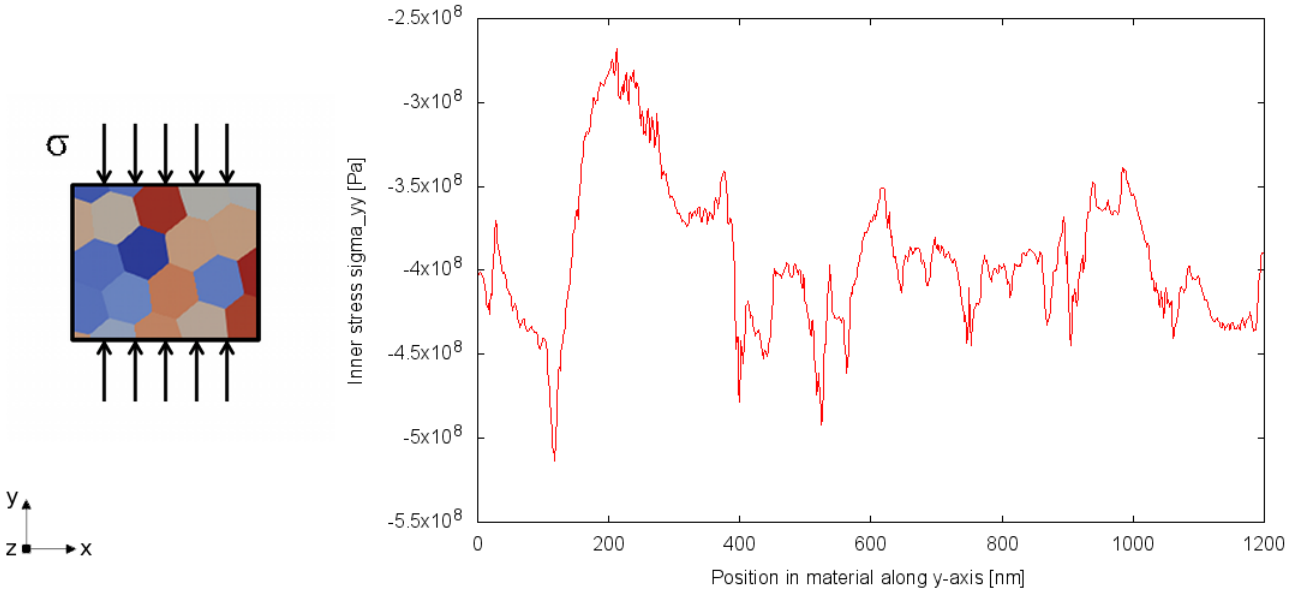

Figure 14: Inner stress of a grain structure. On both sides a force of 400MPa is applied in a compressive manner. Big fluctuations are visible. Eq. 1-4 for linear elasticity are solved.

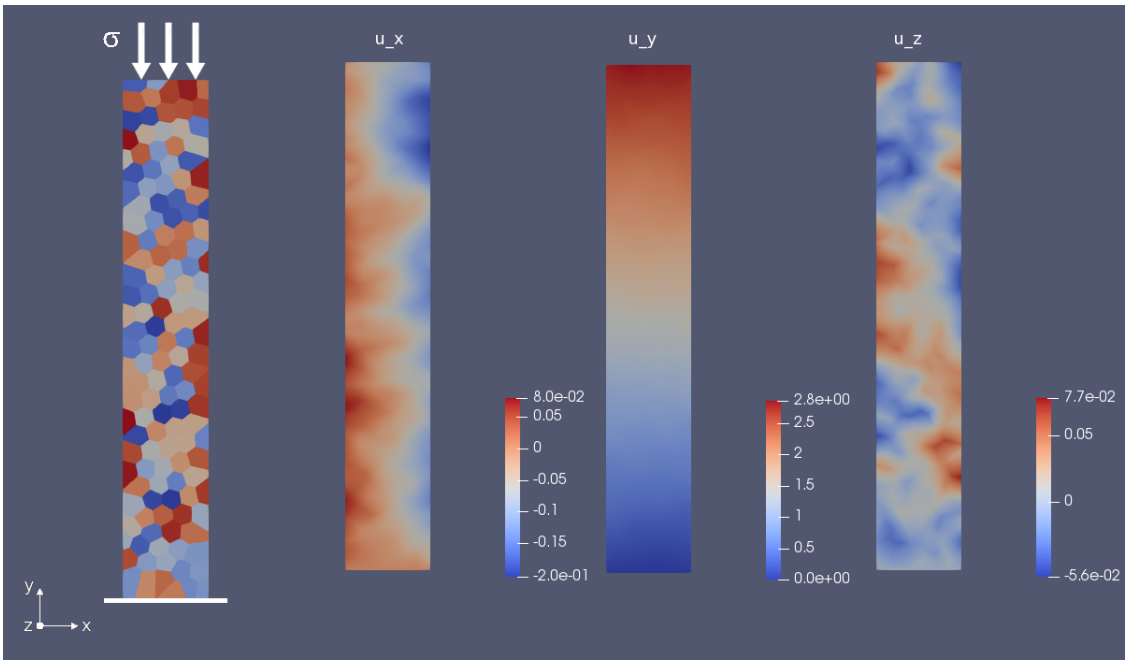

Figure 15: On the left-hand side the setup is shown. The white arrows represent the applied stress (400MPa) and the white bar indicates that the bottom side is fixed by dirichlet boundary conditions. To the right components of displacement field u are shown in the order of u_x, u_y and u_z. The displacement field shows a cloudy distribution because of the randomly oriented grains. Eq. 1-4 for linear elasticity are solved.

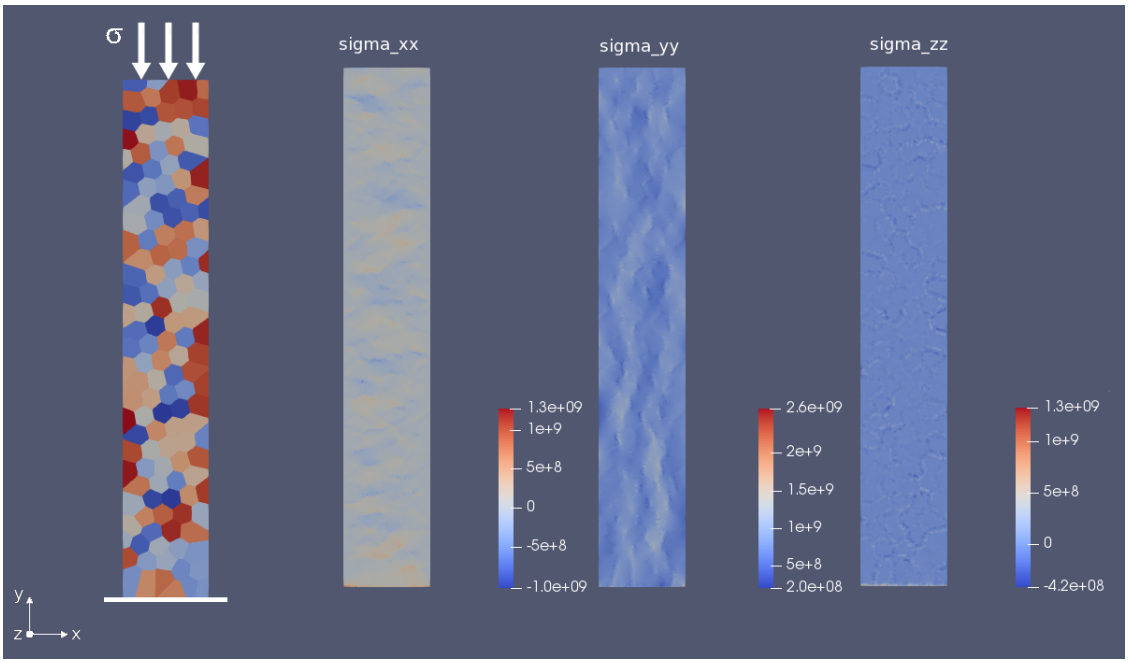

Figure 16: On the left-hand side the setup is shown. The white arrows represent the applied stress (400MPa) and the white bar indicates that the bottom side is fixed by dirichlet boundary conditions. To the right components of stress tensor field σ are shown in the order of σ_{xx}, σ_{yy} and σ_{zz}. Eq. 1-4 for linear elasticity are solved.

3.6 2D Stoner-Wohlfarth model

One of the most simple model for investigating magnetic effects is the so-called Stoner-Wohlfarth model. This two-dimensional model consists of a ferromagnetic material with an uniaxial magnetic anisotropy (easy axis) and a perpendicular directed external magentic field.
As shown by Bergmair et al. [2] the influence of an applied stress (parallel to the external field) in a Stoner-Wohlfarth model is described by a linear material law which saturates at the stress dependent anisotropy field $H_{A\sigma}$. The magnetization in the direction of the external field is given by:

$$m_{\|H}(H,\sigma) = \begin{cases} \frac{H}{H_{A\sigma}} & 0 < H < H_{A\sigma} \\ 1 & H_{A\sigma} \leq H \end{cases}$$

Where the stress dependent anisotropy field is given by:

$$H_{A\sigma} = \frac{2K_{uni} - 3\lambda_s\sigma}{J_s} = \left(1 - \frac{\sigma}{\sigma_c}\right) H_A$$

Here J_s is the saturation polarization, K_{uni} is the anisotropy constant and H_A is the effective field of the uniaxial anisotropy:

$$J_s = \mu_0 M_s$$
$$H_A = \frac{2K_u}{J_s}$$

This is just a simple case of the already derived tensorial effective field of magnetoelasticity:
Since the easy axis is directed perpendicular to the applied uniaxial stress the stress dependent effective anisotropy field is simply given by the effective uniaxial anisotropy field H_A (see 2.2.5)

subtracted by the effective field of magnetoelasticity for the simplified case of uniaxial applied stress:

$$H_{A\sigma} = H_A - \frac{2}{J_s}\frac{3}{2}\lambda_s\sigma = \frac{2K_{uni} - 3\lambda_s\sigma}{J_s}$$

In case of applied stress parallel to easy axis the subtraction changes to an addition.
Comparison of analytical results and numerical results as obtain by FEM-simulation is shown in Fig. 17.
As an orientation value the following characteristic stress is introduced [2]:

$$\sigma_c = \frac{2K_{uni}}{3\lambda_s}$$

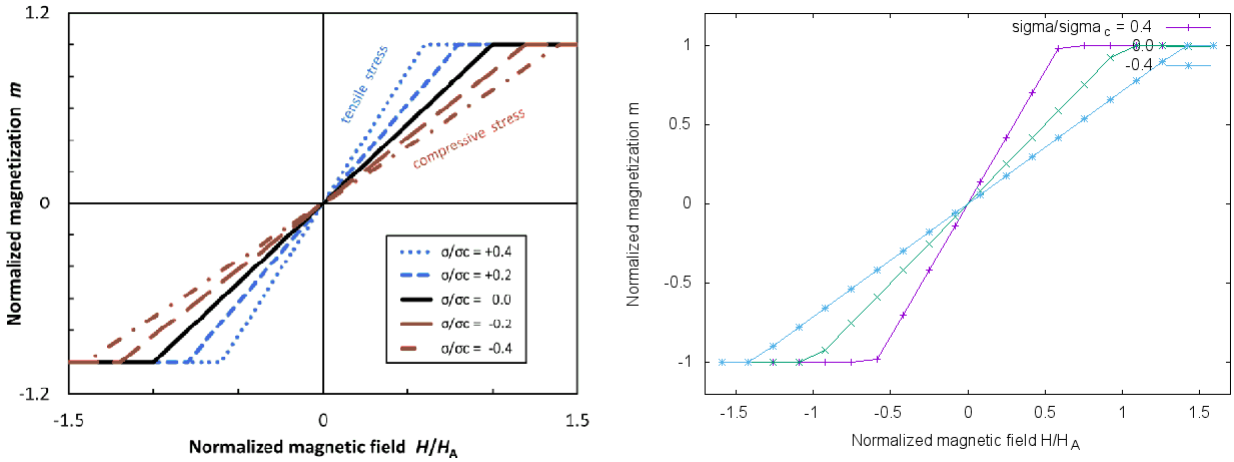

Figure 17: Comparison of analytical results of stress dependent magnetization curves[6] versus numerical results of FEM-simulation. A homogen mesh with constant stress is used. The introduced LLG term for magnetostriction (see Eq. 8) is used. A homogeneous mesh with dimensions 10x10x10 and 1000 cells was used.

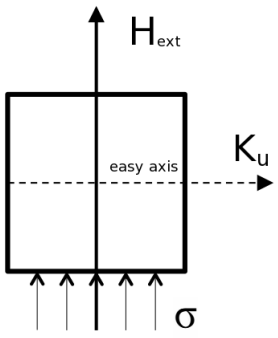

Figure 18: Similar to Stoner-Wohlfarth model an uniaxial magnetic anisotropy (easy axis) is directed perpendicular to an external H-field. A constant stress parallel to H-field is applied.

[6]Image taken from [2]

3.7 Influence of established inner stress on magnetization curve

As pointed out in the previous sections the way how boundary conditions are defined matters and changes what kind of inner stress is established. But since the average of inner stress is always the same for all cases it does not change magnetization curves. This is due to the fact that magnetization curves are measured by taking the average over the whole mesh either way. Results that prove this are shown in Fig. 19. This is indifferent of the dimension of the mesh and does also hold for inhomogeneous structures like grain structures. This is shown in Fig. 20.

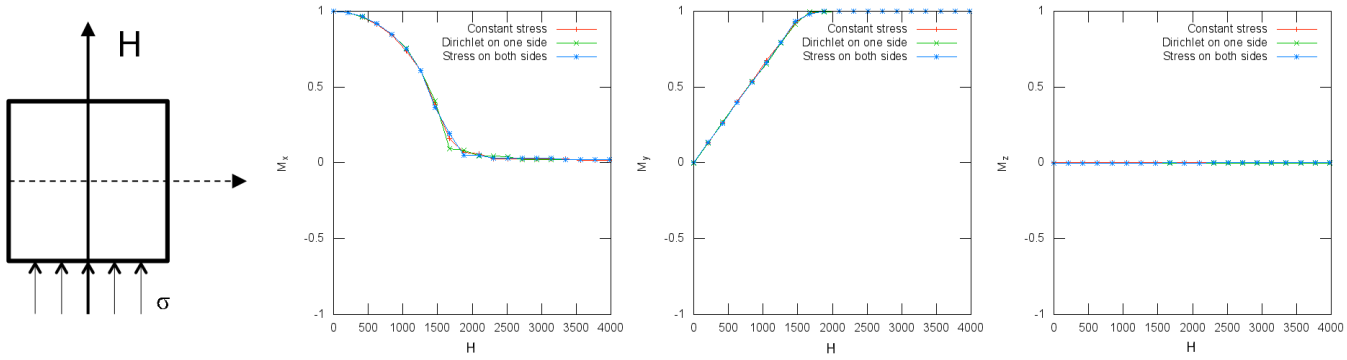

Figure 19: Stress dependent magnetization curves in homogeneous FeCo for different boundary conditions and therefore different fluctuations of inner stress. Clearly in all cases same magnetization curves are measured because specific fluctuations in magnetization get averaged out. Equations for linear elasticity (Eq. 1-4) and magnetostriction (Eq. 8) are solved. A homogenous mesh with dimensions 1200x200x5 (nm) and 1000 cells was used. As applied stress the yield strength of FeCo was chosen (400 MPa).

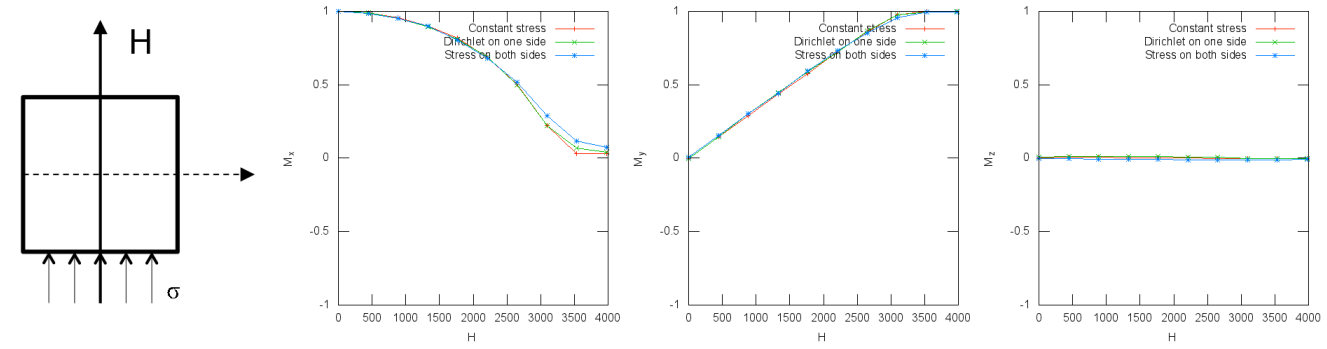

Figure 20: Stress dependent magnetization curves in inhomogeneous (grain structure) FeCo for different boundary conditions and therefore different fluctuations of inner stress. There is no significant deviation in magnetization curves. Same as in homogeneous case the specific fluctuations in magnetization get averaged out. Equations for linear elasticity (Eq. 1-4) and magnetostriction (Eq. 8) are solved. An inhomogenous mesh with dimensions 1200x200x5 (nm), 63885 cells and 139 grains was used. As applied stress the yield strength of FeCo was chosen (400 MPa).

3.8 Stress dependent magnetization curves in homogeneous material

In order to research the effect of magnetostriction in homogeneous material further, magnetization curves for differently oriented applied stresses are obtained.
In the following a directly assigned constant stress is used since it is computed the fastest because no elastic problem has to be solved. Results are shown in Fig. 22.
Firstly it is noted that whether stress is applied parallel to easy axis or external field just changes the sign of magnetoelastic contribution as suggested in previous section.
Accordingly for a stress applied with 45 degrees relative to easy axis a stress independent magnetization curve is measured (which just resembles a superposition of the two former cases).
Consequently, for a stress applied with -45 degress relative to easy axis the contribution of magnetization of magnetoelasticity doubles.
There is still another degree of freedom which is not considered in the four pictured cases and that is the orientation of the FeCo crystal (see Fig. 21). As pointed out in section 2.2.3 the second term vanishes if the crystal is oriented parallel to the coordinate system and no shear stresses are at work. Since λ_{111} of FeCo is far bigger than λ_{100} this makes a huge difference. Therefore, the same four cases are computed with the FeCo crystal being rotated in a way that the body diagonal is parallel to the coordinate system. Results are shown in Fig. 23.

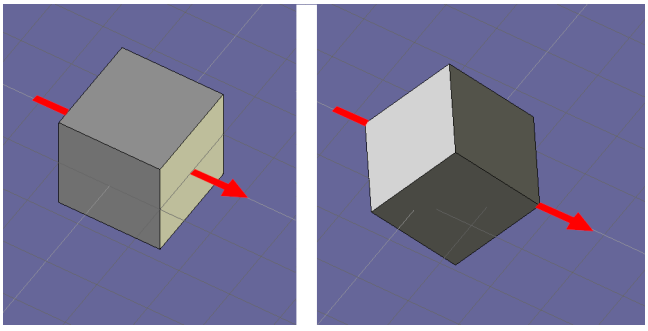

Figure 21: For the left-hands-side the cubic crystal is oriented parallel to the coordinate system (minimal magnetostriction). For the right-hand-side the crystal is rotated and the same force (indicated by the red arrow) acts along the body diagonal of the crystal (maximal magnetostriction).

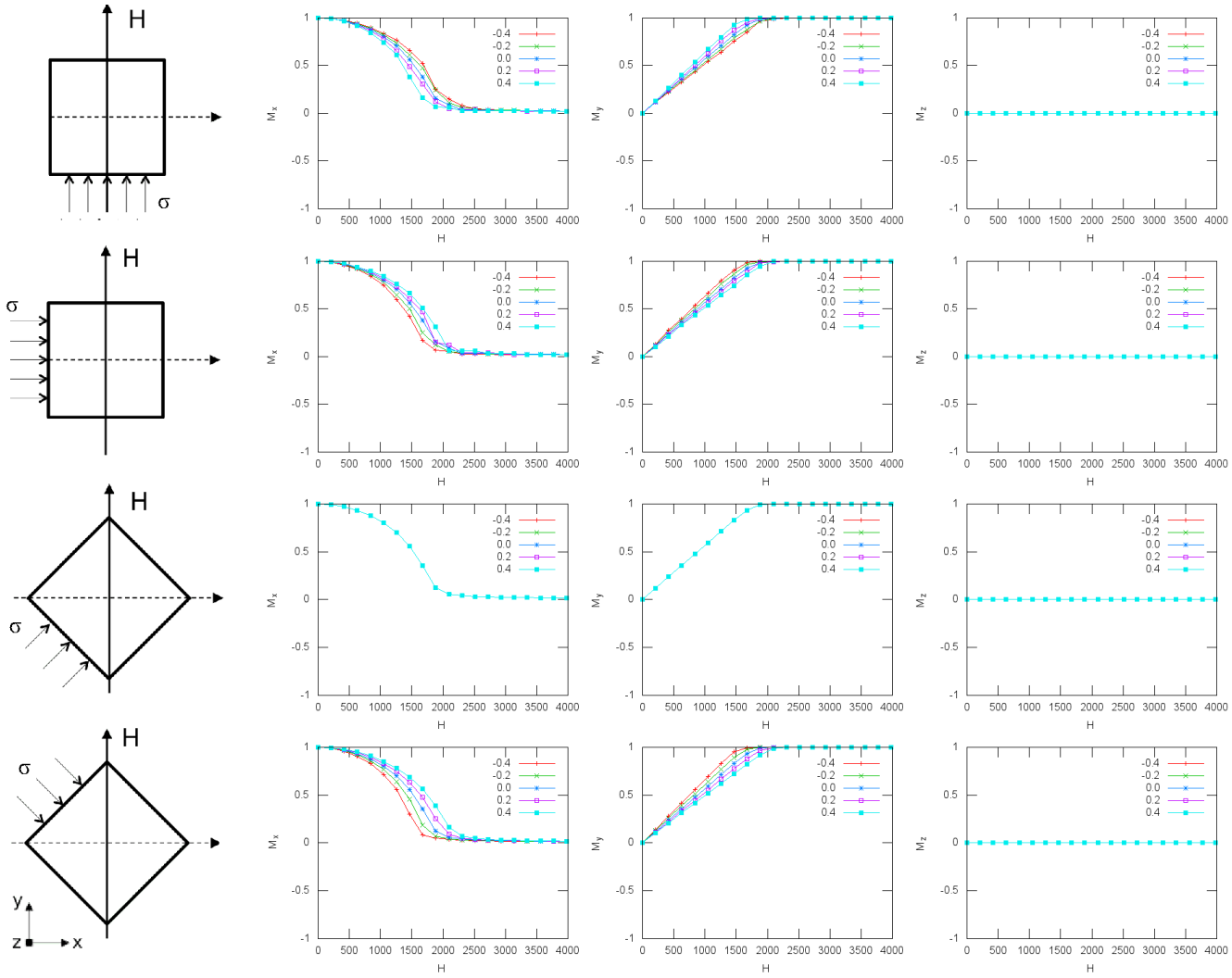

Figure 22: **Minimal magnetostriction (see Fig. 21)**: Stress dependent magnetization curves in homogeneous FeCo for different stresses varied in orientation relative to the easy axis (dotted line) and magnitude. The homogeneous material is rotated in a way to show minimal magnetostriction (no shear stresses). A constant stress and Eq. 8 is used. A homogeneous mesh with dimensions 1200x200x5 (nm) was chosen. As applied stress the characteristic stress σ_c multiplied by the number given in the plot was used. Additional simulation parameters: $K_{uni} = 1920$, $J_s = 1T$, $A_{ex} = 2 \cdot 10^{-11} \frac{J}{m}$.

.

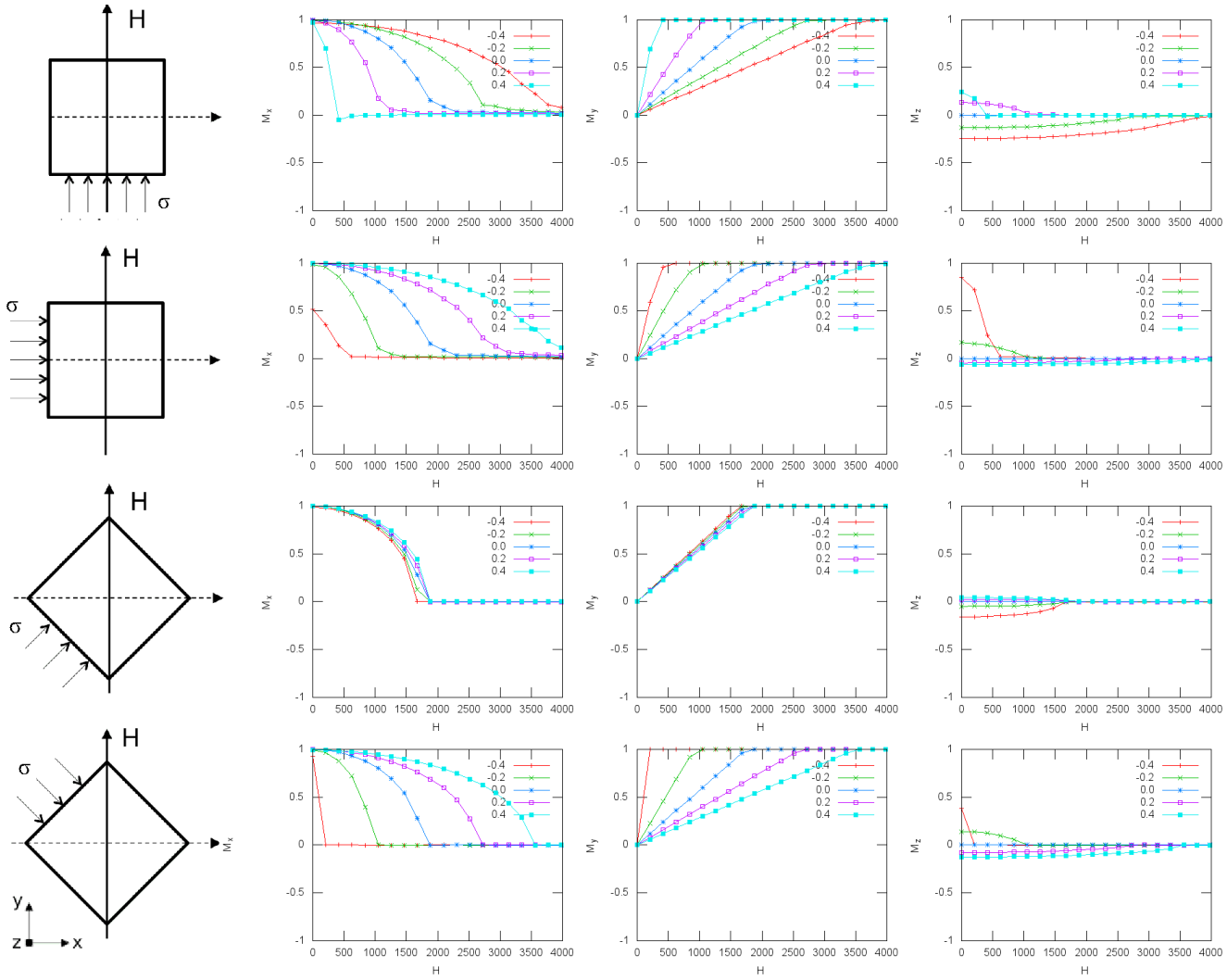

Figure 23: **Maximal magnetostriction (see Fig. 21)**: Stress dependent magnetization curves in homogeneous FeCo for different stresses varied in orientation relative to the easy axis and magnitude. The homogeneous material is rotated in a way to show maximal magnetostriction (high shear stresses). A constant stress and Eq. 8 is used. A homogeneous mesh with dimensions 1200x200x5 (nm) was chosen. As applied stress the characteristic stress σ_c multiplied by the number given in the plot was used. Additional simulation parameters: $K_{uni} = 1920$, $J_s = 1T$, $A_{ex} = 2 \cdot 10^{-11} \frac{J}{m}$.

.

3.9 Stress dependent magnetization curves in inhomogeneous materials

Similar to the previous section four test cases with different orientation of applied stress and external magnetic field are build. Contrarily to the previous section an inhomogeneous material is used.
It has already been shown that all types of stress result in the same magnetization curves. Therefore, a constant stress is assigned and grains are randomly oriented in terms of stiffness and magnetostriction.
The resulting magnetization curves are qualitatively identical (see Fig. 24). In terms of the magnitude of magnetostriction an average between the homogenous minimal case (see Fig. 22) and homogeneous maximal case (see Fig.23) seems to be obtained.

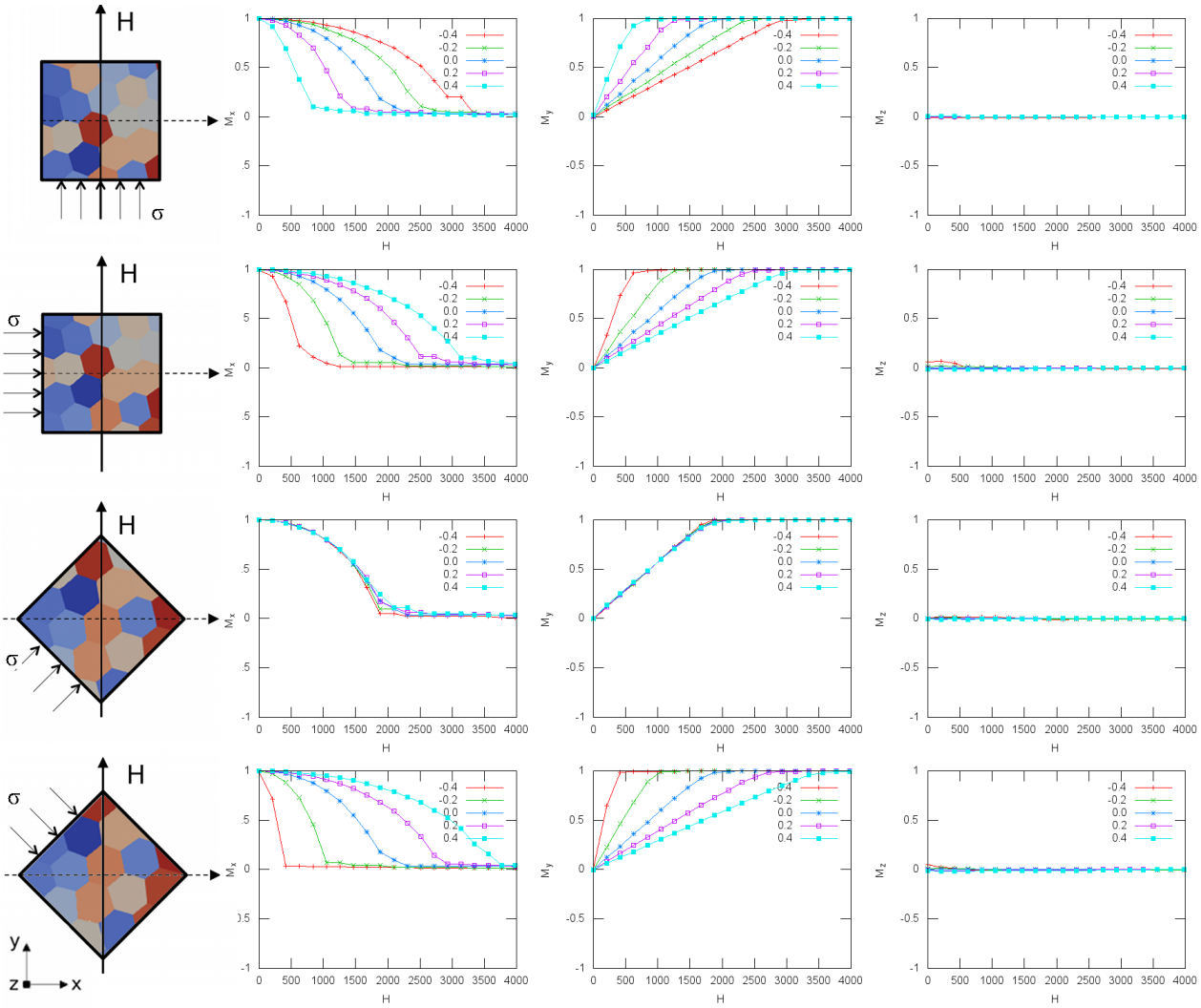

Figure 24: Stress dependent magnetization curves in polycrystalline FeCo for different stresses varied in orientation relative to the easy axis and magnitude. A constant stress and Eq. 8 is used. A inhomogeneous mesh with dimensions 1200x200x5 (nm), 63885 cells and 139 grains was chosen. As applied stress the characteristic stress σ_c multiplied by the number given in the plot was used. Additional simulation parameters: $K_{uni} = 1920$, $J_s = 1T$, $A_{ex} = 2 \cdot 10^{-11} \frac{J}{m}$, grain diameter = 40nm.

3.10 Effective magnetostriction

For polycrystalline materials rotation of the stiffness but also magnetostriction constants have to be considered.
Instead of rotating the magnetostriction tensor for each grain individually an effective magnetostriction for the whole material can be approximated as shown in Section 2.2.4.
To investigate if these new methods will lead to better results than the commonly used saturation magnetostriction λ_s a test case like in the previous section is used. Then the magnetization curves for different approximation methods are computed. Unfortunately as displayed in Fig. 25 these newly introduced approximation methods for magnetostriction yield no better results then the commonly used saturation magnetostriction but still results are very close to the real curves in the case of iron-cobalt.

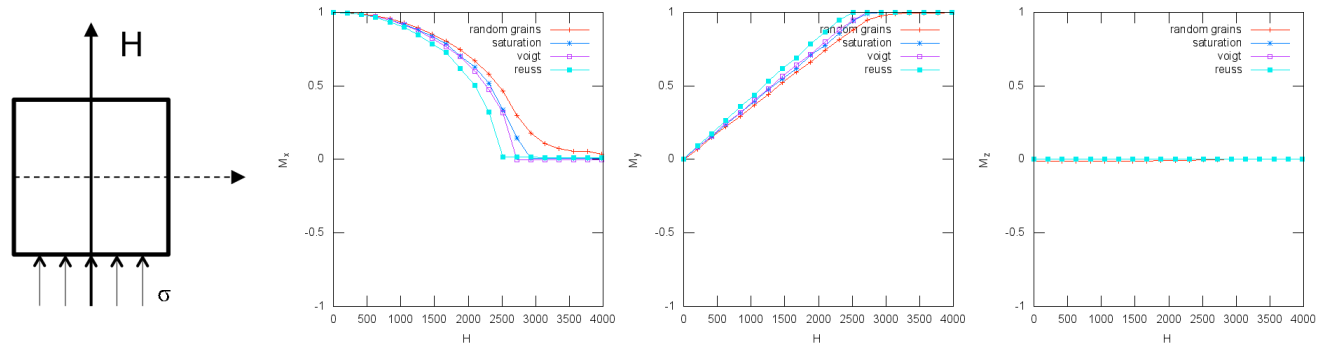

Figure 25: Stress dependent magnetization curves in a homogeneous (monocrystalline) material of FeCo for different approximated effective magnetostriction constants (saturation magnetostriction, Voigt Method, Reuss Method) and for comparison with the "real" magnetization curve of randomly oriented grains. A constant stress and Eq. 8 is used.

4 Discussion and Outlook

In this work many important observations have been made: First of all, both thermal stress and surface pressure result in different inner stress states. But in terms of magnetization curves no significant difference is observed. As a consequence, for simple cases and geometries it is sufficient to assign a constant inner stress and no linear elasticity solver has to be used. This holds for homogeneous or monocrystalline as well as inhomogeneous or polycrystalline materials. Further, in the case of an uniaxial stress, magnetostriction can be expressed as a simple unixial anisotropy with an axis along the applied stress and a specific stress dependent constant as derived in Section 2.2.5.

Furthermore polycrystalline materials can be approximated with effective stiffness or compliance tensors. The same approach can be used for magnetostriction which is a fourth-order tensor as well. Results of the Voigt Method applied on magnetostriction are similar to the commonly used saturation magnetostriction. Unfortunately no improvement in accuracy could have been observed.

The most important observation though was a massive increase of magnetostriction if stress was applied in a way that iron-cobalt crystals experience a shear stress.

This is obviously due to the fact that magnetostriction along the body diagonal λ_{111} is much higher in contrast to the magnetostriction along the side length of the crystal λ_{100}.

This fact can be utilized to reduce magnetostrictive effects in materials. As shown in Fig. 22 and Fig. 23 a specific external stress of $0.2 \cdot \sigma_c$ leads to an increase in susceptibility of 5% if the single crystal is oriented parallel to the external stress. On the contrary the same external stress leads to an increase of 64% in susceptibility if the stress is aligned along the body diagonal of the single crystal. For the polycrystalline case of randomly oriented grains an increase of 46% in susceptibility was observed. This effect in polycrystalline materials can be reduced by making sure that all crystals are at least on a plane parallel to the uniaxial stress. This reduces overall shear stresses and therefore magnetostrictive effects. Manufacturing the free layer for GMR sensors in that way should be further studied.

In addition, all computations done in this work can of course be carried out for Nickel (Ni) which, in contrast to FeCo, has a positive magnetostriction and is used in many applications for that reason. It might be possible to construct a GMR sensor consisting of alternating Ni and FeCo slices or layers to obtain a very small overall magnetostriction. Similar ideas but with different objectives have already been studied [12].

References

[1] A. Bachleitner-Hofmann, B. Bergmair, T. Schrefl, A. Satz, and D. Suess. Soft magnetic properties of thin nanocrystalline particles due to the interplay of random and coherent anisotropies. *IEEE Transactions on Magnetics*, 53(11):1–6, Nov 2017. ISSN 0018-9464. doi: 10.1109/TMAG.2017.2695580.

[2] B. Bergmair, T. Huber, F. Bruckner, C. Vogler, M. Fuger, and D. Suess. Fully coupled, dynamic model of a magnetostrictive amorphous ribbon and its validation. *Journal of Applied Physics*, 115(2):023905, 2014. doi: 10.1063/1.4861735. URL https://doi.org/10.1063/1.4861735.

[3] S. Chikazumi, S. Chikazumi, and C. Graham. *Physics of Ferromagnetism*. International Series of Monogr. Clarendon Press, 1997. ISBN 9780198517764. URL https://books.google.at/books?id=PMURDAAAQBAJ.

[4] M. de Jong, W. Chen, T. Angsten, A. Jain, R. Notestine, A. Gamst, M. Sluiter, C. Krishna Ande, S. van der Zwaag, J. J. Plata, C. Toher, S. Curtarolo, G. Ceder, K. A. Persson, and M. Asta. Charting the complete elastic properties of inorganic crystalline compounds. *Scientific Data*, 2:150009 EP –, Mar 2015. URL https://doi.org/10.1038/sdata.2015.9. Data Descriptor.

[5] U. Fourier. *Magnetism: Fundamentals, Materials and Applications*. Magnetism. Springer New York, 2002. ISBN 9781402072222. URL https://books.google.at/books?id=2w840s028pAC.

[6] A. Jain, S. P. Ong, G. Hautier, W. Chen, W. D. Richards, S. Dacek, S. Cholia, D. Gunter, D. Skinner, G. Ceder, and K. a. Persson. The Materials Project: A materials genome approach to accelerating materials innovation. *APL Materials*, 1(1):011002, 2013. ISSN 2166532X. doi: 10.1063/1.4812323. URL http://link.aip.org/link/AMPADS/v1/i1/p011002/s1\&Agg=doi.

[7] P. Kelly. Mechanics lecture notes: An introduction to solid mechanics. URL http://homepages.engineering.auckland.ac.nz/~pkel015/SolidMechanicsBooks/Part_I/index.html.

[8] H. Kronmüller and S. Parkin. *Handbook of magnetism and advanced magnetic materials: Spintronics and magnetoelectronics*. Handbook of Magnetism and Advanced Magnetic Materials. John Wiley & Sons, 2007. URL https://books.google.at/books?id=N-rXAAAAMAAJ.

[9] C.-Y. Liang, S. M. Keller, A. E. Sepulveda, A. Bur, W.-Y. Sun, K. Wetzlar, and G. P. Carman. Modeling of magnetoelastic nanostructures with a fully coupled mechanical-micromagnetic model. *Nanotechnology*, 25(43):435701, oct 2014. doi: 10.1088/0957-4484/25/43/435701. URL https://doi.org/10.1088%2F0957-4484%2F25%2F43%2F435701.

[10] N.-J. Park, H. J. Bunge, H. Kiewel, and L. Fritsche. Calculation of effective elastic moduli of textured materials. *Textures and Microstructures*, 23, 01 1995. doi: 10.1155/TSM.23.43.

[11] F. Project. The fenics computing platform. URL https://fenicsproject.org/.

[12] E. Quandt, A. Ludwig, J. Betz, K. Mackay, and D. Givord. Giant magnetostrictive spring magnet type multilayers. *Journal of Applied Physics*, 81(8):5420–5422, 1997. doi: 10.1063/1.364558. URL https://doi.org/10.1063/1.364558.

[13] SuessCo. Welcome to magnum.fe's documentation! URL http://micromagnetics.org/magnum.fe/.

[14] A. Ugural and S. Fenster. *Advanced Strength and Applied Elasticity*. Pearson Education, 2003. ISBN 9780132440523. URL https://books.google.at/books?id=fvQy2PdAuHIC.

[15] A. Visintin. On landau-lifshitz' equations for ferromagnetism. *Japan Journal of Applied Mathematics*, 2:69–84, 06 1985. doi: 10.1007/BF03167039.